Novel Roles of SOCS3 as a Tumour Suppressor

Research Master's Thesis

Chloe Jewers BSc (Hons)

Lancaster University

Biomedical and Life Sciences

April 2024

I, Chloe Jewers, confirm that the work presented in this thesis is my own and has not been submitted in substantially the same form for the award of a higher degree elsewhere. Where information has been derived from other sources, I confirm this has been indicated in the thesis.

Submitted in part fulfilment of the requirements for the degree of Research Masters

Abstract

Cancer is a collection of diseases that were responsible for approximately ten million deaths in 2020. Colorectal cancer (CRC) is the third most common type of cancer; it occurs following the transformation of normal epithelial cells to adenocarcinoma which can eventually result in metastasis. Treatments are continuously being researched and developed, with immunotherapy becoming an increasingly common area of research against cancer. The enzyme indoleamine 2,3-dioxygenase (IDO) has been identified as a cause of tumour immune tolerance through the creation of a tryptophan-starved state in cells. Hence, blockers to IDO have been studied to test their efficacy in treating cancers. IDO blocker Epacadostat has been found to be effective in mice but has proven to be variable in success in human trials. Another IDO blocker under investigation is 1-methyl-D-tryptophan (1-MT). This project aimed to investigate the impact of the loss of tumour suppressor, SOCS3, on 1-MT treatment due to its ability to regulate IDO expression. SOCS3 silencing has been associated with some human cancers, therefore this study used conditional intestinal epithelial SOCS3 knockout mice (IECS3-/-) to recapitulate the loss of SOCS3 in intestinal adenocarcinoma. An azoxymethane/ dextran sodium sulphate (AOM/DSS) model was used to induce colon cancer and conditional knockout, or wild-type mice were administered either 1-MT or water. Analysis of the intestinal macrophages was performed using immunohistochemistry, IDO activity assessed using HPLC, and cell culture techniques to investigate impact of 1-MT in vitro. A decrease in M1 pro-inflammatory macrophages was found in the colon of IECS3 -/- 1-MT treated mice, and an increase in CD206+ IBA1- cells (potential immature dendritic cells (IDCs)) in IECS3-/- H_2O treated mice. These findings indicate that a SOCS3 deficiency may play a role in reducing the efficacy of 1-MT immunotherapy treatment, presenting itself as a potential biomarker that could help identify patients who are likely to see improved prognosis following IDO-inhibitor treatment.

Table of Contents

Acknowledgements

I would like to acknowledge and express gratitude to my supervisor Dr Rachael Rigby for all her help, guidance, and support throughout my master's project. I would also like to thank Dr Jack Martin for his supervision and training in HPLC, and Dr Alejandra Zarate-Potes for providing the resources to help me analyse the HPLC data.

I am also extremely grateful to Dr Cheryl Hawkes for her help and insight into immunohistochemistry and advice which helped me develop and optimise the method. Additionally, I thank Dr Elisabeth Shaw for her training and guidance in fluorescence microscopy.

Lastly, I would like to thank my family for their support and motivation throughout the entire project.

Glossary

AA: 3-Hydroxyanthranilic Acid

ACN: Acetonitrile

AF: Alexa Fluor

ANOVA: One-Way Analysis of Variance

APC: Adenomatous Polyposis Coli

APES: Aminopropyltriethoxysilane

BSA: Bovine Serum Albumin

CD8: Cluster of Differentiation 8

CD206: Cluster of Differentiation 206

C-FLIP: Cellular FLICE-like Inhibitory Protein

CIS: Cytokine-inducible SRC Homology 2 (SH2)-Domain-Containing Proteins

CO_2: Carbon Dioxide

CRC: Colorectal Cancer

CTLA-4: Cytotoxic T-Lymphocyte Associated-Antigen 4

DAD: Diode Array Detector

DAPI: 4',6-diamidino-2-phenylindole

DC: Dendritic Cell

dH_2O: Distilled Water

DSS: Dextran Sodium Sulphate

EDTA: Ethylenediaminetetraacetic acid

EtOH: Ethanol

FBS: Fetal Bovine Serum

FIT: Faecal Immunochemical Test

Gp130: glycoprotein 130 kDa

HCl: Hydrochloric Acid

HPLC: High-Performance Liquid Chromatography

HSD: Honestly Significant Difference

H_2O: Water

IBA-1: Ionized Calcium Binding Adaptor Molecule 1

ICI: Immune Checkpoint Inhibitor

IDO: Indoleamine 2,3-dioxygenase 1

IDC: Immature Dendritic Cell

IEC: Intestinal Epithelial Cell

IECS3 -/-: Intestinal Epithelial Cell SOCS3 k/o

IgG: Immunoglobulin G

IL: Interleukin

IFN-γ: Interferon-gamma

iNOS: Inducible Nitric Oxide Synthase

JAK: Janus Kinase

JAK-STAT: Janus Kinase and Signal Transducer and Activator of Transcription

KIR: Killer Inhibitory Receptors

K/O: Knockout

KYN: Kynurenine

KYNA: Kynurenic Acid

LOD: Limits of Detection

LPS: Lipopolysaccharides

MHC: Major Histocompatibility Complex

NK: Natural Killer

NKG2D: Natural Killer Group 2D

PBS: Phosphate-buffered Saline

PCR: Polymerase Chain Reaction

PD-L1: Programmed Death-Ligand 1

PD-1: Programmed Cell Death Protein-1

PFA: Paraformaldehyde

PMA: Phorbol 12-Myristate 13-Acetate

RPMI: Roswell Park Memorial Institute

SDS-PAGE: Sodium Dodecyl Sulphate-Polyacrylamide Gel Electrophoresis

SEM: Standard Error of the Mean

SH2: SRC homology 2

SOCS: Suppressor of Cytokine Signalling

SOCS3: Suppressor of Cytokine Signalling 3

STAT3: Signal Transducer and Activator of Transcription 3

TBS: Tris-Buffered Saline

TGF-β: Transforming Growth Factor-β

TGS: Tris-Glycine-SDS

TFA: Trifluoroacetic Acid

TIL: Tumour Infiltrating Lymphocyte

T-reg: Regulatory T-Cell

TRP: Tryptophan

Wt: Wildtype

VEGF: Vascular Endothelial Growth Factor

VEGFR: Vascular Endothelial Growth Factor Receptor

1-MT: 1-Methyl-D-Tryptophan

3-HAA: 3-Hydroxyanthraniliac Acid

3-HK: 3-Hydroxykynurenine

1. Literature Review

1.1. Introduction to Cancer

Cancer is a term used to describe a collection of more than two hundred diseases that can affect any part of the body (Hassanpour & Dehghani, 2017). However, it is specifically defined as the abnormal proliferation of cells, which occurs in an unregulated way and results in the development of a malignant tumour. This can later result in metastasis, which is when the cancer cells invade and colonise other parts of the body through the blood and lymphatic system (Alzahrani et al., 2021). Worldwide, it is responsible for approximately ten million deaths in 2020, making it one of the leading killers (World Health Organization, 2022).

The development of cancer is characterised by a genetic change in cells causing them to evade apoptosis or divide in an uncontrolled manner. These genetic changes, also known as mutations, can occur as a result of chemical, physical, and biological carcinogens. Exposure to these carcinogens is known to increase the risk of developing cancer through the process of carcinogenesis, which results in the activation of oncogenes/ deactivation of tumour suppressor genes (Alzahrani et al., 2021). Furthermore, cancer predisposition genes, a group of germ line inherited mutant alleles, increase the risk of cancer development in an individual. An example of this is the BRCA1 gene which, when mutated, leads to the development of breast cancer in 55-65% of cases (National Cancer Institute, 2022). Cancer incidence is known to increase significantly with age, due to the increase in chance of mutations over time, along with the decreased ability to repair cells (White et al., 2014). There are four main groups most cancers will fall into, these include carcinomas, sarcomas, leukaemia, and lymphomas. Carcinomas are derived from epithelial cells, sarcomas are derived from skeletal and connective tissue, leukaemia from bone marrow stem cells and lymphomas from immune cells (Alzahrani et al., 2021).

Cancer cells behave differently from normal cells in several ways. Hanahan and Weinberg (2000) developed six hallmarks to characterise cancer cells, these include the ability to resist

apoptosis, induce angiogenesis, enable replicative immortality, evade growth inhibitory signals, sustain proliferative signalling, and activate invasion and metastasis (Figure 1).

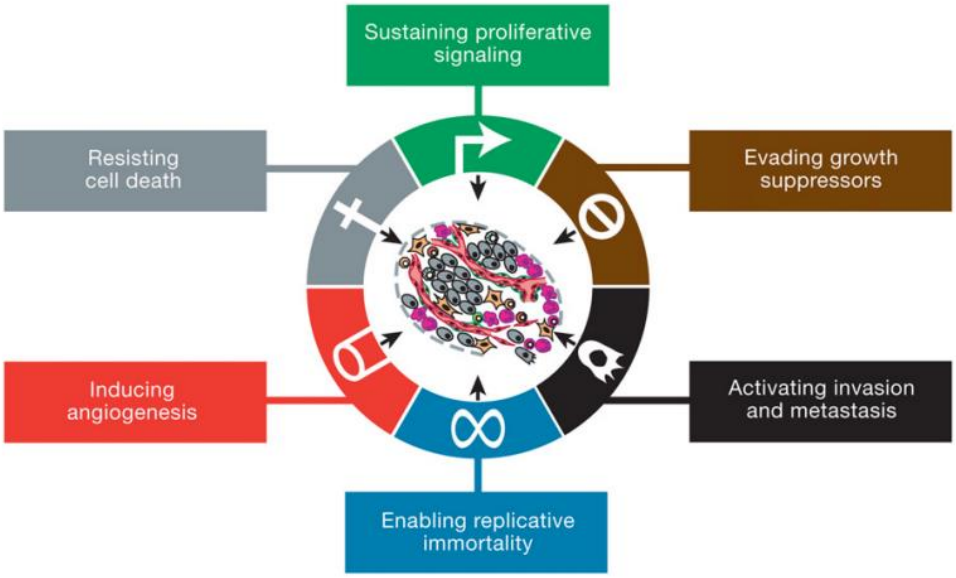

Figure 1. Initial six hallmarks of cancer as described by Hanahan and Weinberg, 2000.

Additional hallmarks and enabling characteristics were described in 2011, these include the ability to evade immune destruction and deregulate cellular energetics (Figure 2). Together, these characteristics define cancerous cells.

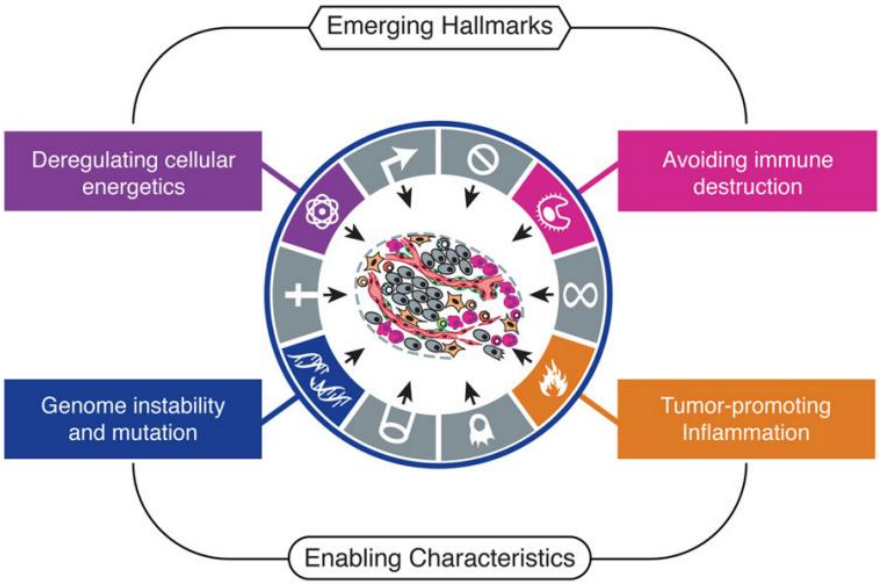

Figure 2. Further two hallmarks of cancer as described by Hanahan and Weinberg, 2011.

The three most common cancer types are: breast, lung, and colorectal cancer (CRC) and these together accounted for over 6 million cases in 2020 (World Health Organization, 2022).

1.2. Colorectal Cancer

The colon is one of the four parts that make up the large intestine. It is the longest part, comprised of an ascending region, a transverse region, a descending region, and a sigmoid region (Figure 3) (Lin et al., 2016). Its main function is to remove water and nutrients from partially digested food and to transport waste material out of the body (National Cancer Institute, 2023).

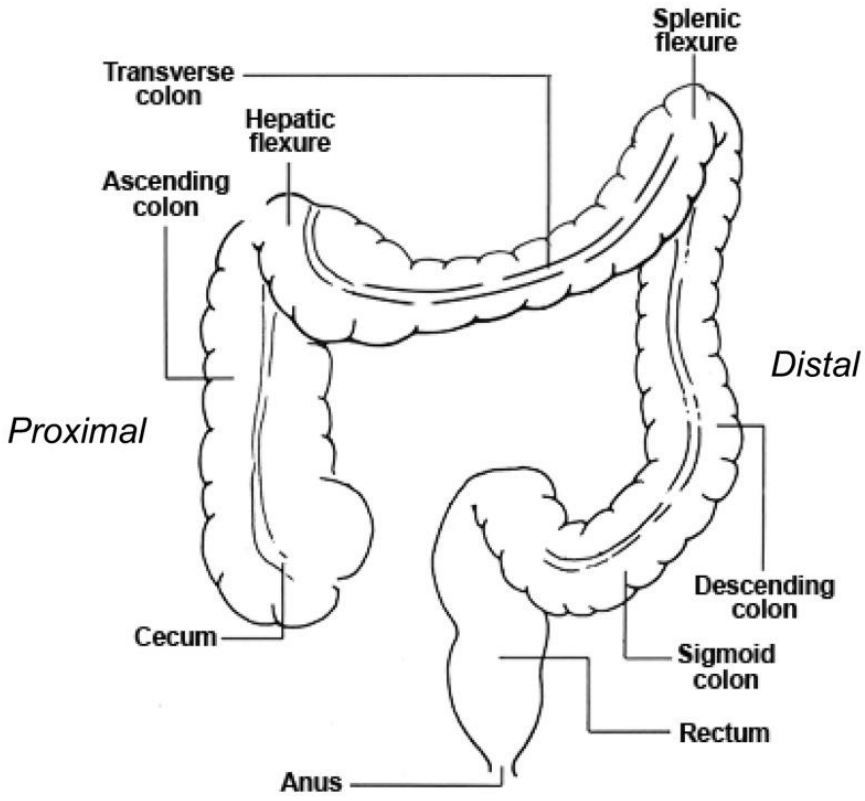

Figure 3. Structure of the colon (sourced from Lin et al., 2016).

CRC can be defined as the transformation of normal epithelial cells in the colon/ rectum to a precancerous adenoma which eventually forms a carcinoma and metastasis can occur.

In the UK, between the ages of 60 and 74, screening for bowel cancer is completed using the

faecal immunochemical test (FIT), people at high risk of developing CRC can be screened at a younger age via a colonoscopy to detect cancer in its early stages making treatment more likely to be successful (Cancer Research UK, 2022).

CRC is the third most common type of cancer, accounting for approximately 1.93 million cancer cases, and was the second most common cancer resulting in mortality in 2020 (World Health Organization, 2022). CRC cases have become more prominent over the last few decades, likely due to an increase in risk factors such as smoking, obesity and an increasing ageing population (Kuipers et al., 2015).

A model well characterised in cancer research is that produced by Fearon and Vogelstein in 1990. It proposed that the development of CRC occurs as a result of genetic and epigenetic changes over time, resulting in phenotypic changes to the colon (Figure 4). It showed that malignant carcinomas arise from pre-existing benign adenomas already present in the colon/rectum and that their progression is a result of a number of genetic changes in oncogenes and tumour suppressors over time.

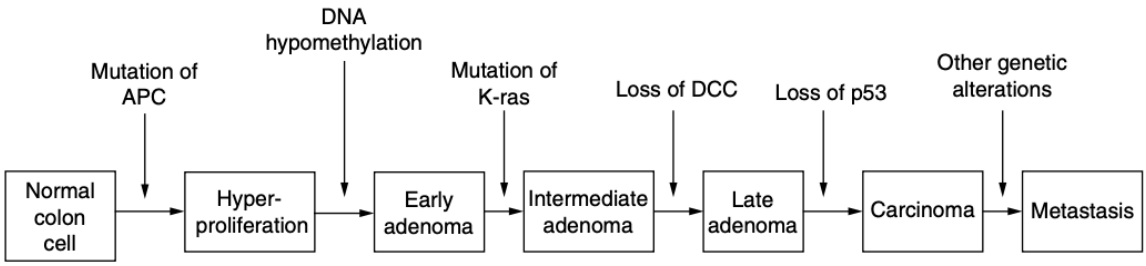

Figure 4. Progression of CRC from normal colon epithelium to abnormal crypt formation, then advanced polyp formation and finally a metastatic tumour, a genetic model initially proposed by Fearon and Vogelstein (1990) (sourced from Martinez et al., 2003). *An initial mutation of adenomatous polyposis coli (APC) (a known tumour suppressor gene) is what is thought to be the initiation event and is followed by many other genetic and epigenetic changes.*

However, in more recent years, mutations at other loci have been identified in addition to those mentioned above that are thought to be additional or alternative in the development of CRC (Ilyas & Tomlinson, 1996).

1.3. The Tumour Immune Environment

Prominent cells in the innate anti-tumour response are natural killer (NK), tumour infiltrating lymphocytes (TILs), and macrophages (M1 specifically). NK cells have two types of receptors that either activate or inhibit their function. Activating receptors include natural killer group 2D (NKG2D) which bind to ligands that are highly expressed on cancerous cells and allow the release of cytotoxic molecules (Pernot et al., 2014). Killer inhibitory receptors (KIR) lead to NK activation when not bound by major histocompatibility complex (MHC)-class 1 molecules, a response likely induced by the tumour's ability to reduced MHC-1 expression (Pernot et al., 2014). In addition to this, NK cells can secrete pro-inflammatory cytokines such as interferon-gamma (IFN-γ), inducing cytotoxic effects on the tumour (Terme et al., 2013). In CRC, a better prognosis was found when more NK cells had infiltrated the tumour (Coca et al., 1997).

TILs, made of T, B, NK cells and macrophages recognise and invade tumours. They play an important role in the anti-tumorigenic response and are being extensively studied as a potential target to enhance immunotherapies against several cancers, including CRC (Kazemi et al., 2022).

Two subtypes of macrophages, M1 and M2, are significant modulators of anti-tumour immunity with different effects on cancer progression (Figure 5). M1 macrophages produce pro-inflammatory molecules such as IL-6 which help activate other immune cells and promote cytotoxic effects in the tumour (Pernot et al., 2014). Alternatively, M2 macrophages, which are primarily involved in wound healing, contribute to tumour growth through their anti-inflammatory effects (Pernot et al., 2014). Infiltration with macrophages in CRC has been found to correlate with a better prognosis (Edin et al., 2013). Specifically, Edin et al (2012) found that M1 macrophages were favourable for achieving this effect in CRC.

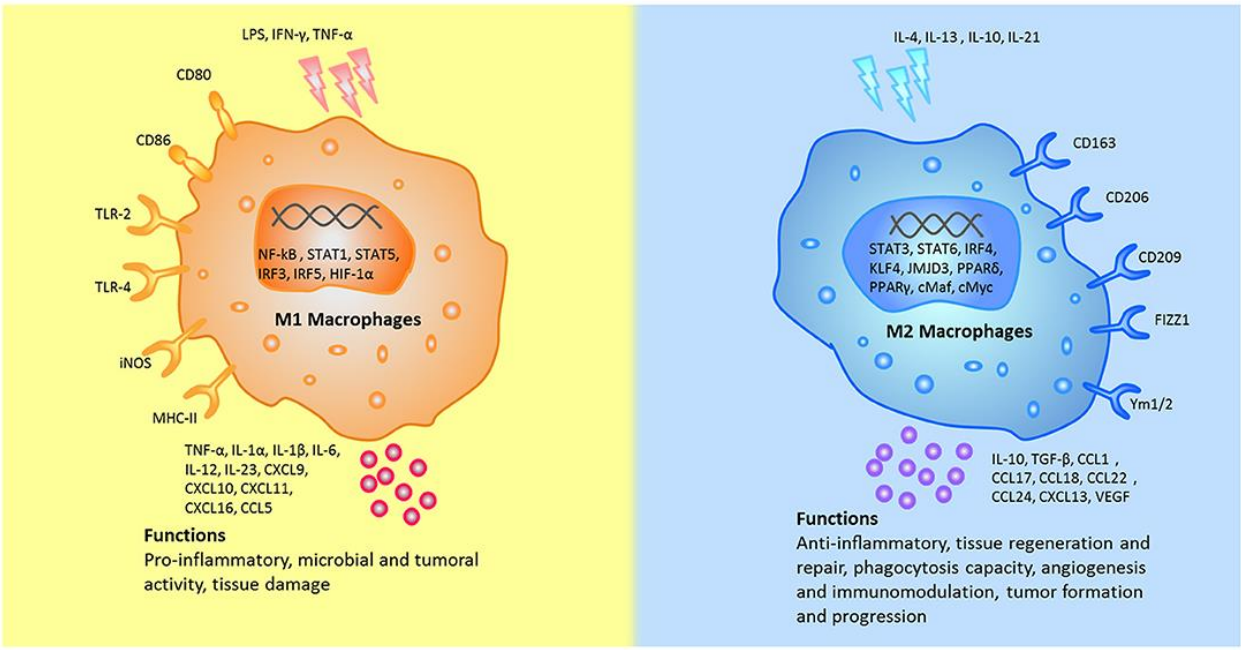

Figure 5. Key features of M1 and M2 macrophages including their surface markers, biological functions, and secreted cytokines (Yao et al., 2019).

Despite these responses, CRC has the ability to evade the immune system through mechanisms including the secretion of immunosuppressive cytokines, downregulation of MHC-1 and induction of regulatory T-cells (T-regs) (Pernot et al., 2014).

Immunosuppressive cytokines, such as IL-10, transforming growth factor-β (TGF-β) and vascular endothelial growth factor (VEGF) all contribute to the prevention of dendritic cells (DCs) becoming mature and they induce the production of T-regs instead of T-lymphocytes (Pernot et al., 2014). CRC tumour cells have the ability to evade apoptosis by inducing cellular FLICE-like inhibitory protein (C-FLIP), an anti-apoptotic molecule or by preventing the expression of FAS, a death receptor (Pernot et al., 2014).

MHC-1 is important in ensuring immune activation as part of the antigen presentation pathway and is expressed on all nucleated cells (Hewitt, 2003). MHC-1 was found to be downregulated in over 70% of CRC tumours (Menon et al., 2002) and in some cases was absent on tumour cells (Cabrera et al., 2003). Pernot et al. (2014) found that reduced expression of MHC-1 led to greater immune survival in CRC tumours, suggesting that the

cancer cells were able evade to T-cell immune surveillance. This is supported by Sourav & Girdhari, 2017, where reduction of MHC-1 expression decreased the tumour's elimination by cluster of differentiation 8 (CD8) T-cells, which in turn upregulates activation of NK cells as there is reduced binding of MHC-1 to the killer inhibitory receptor.

Finally, the induction of T-regs enables immune evasion in tumours as it utilises the body's natural defence against immune disorders (Pernot et al., 2014). This is achieved through the secretion of IL-10, TGF-β and metabolites, including adenosine, which are immunosuppressive (Pernot et al., 2014). CRC has been recognised as a tumour which presents increased T-reg presence, within the blood and tumour (Sellitto et al., 2011). T-regs are involved in many pathways that could explain their accumulation in tumours (Tanchot et al., 2013). Alongside immunosuppressive cytokines, chemokine production and VEGF secretion promotes T-regs (Pernot et al., 2014).

The immunotolerant nature of CRC prevents the body's natural defences from eradicating the tumour. Therefore, medical treatment is required to treat or cure the disease.

1.4. Immunotherapy

Currently, the primary therapeutic for CRC is surgical removal, and in cases where this is not possible or the tumour has metastasized, chemotherapy and radiotherapy are administered (Kumar et al., 2023). Immunotherapy is an emerging cancer treatment which aims to enhance and/ or activate the body's immune system to fight cancer (Kumar et al., 2023).

Specific immunotherapeutic approaches include using monoclonal antibodies to target VEGF and VEGF receptor (VEGFR), immune checkpoint inhibitors (ICI) and adoptive cell therapy. Monoclonal antibodies such as bevacizumab can be used in such a way that the function of VEGF, when bound to its receptor, is inhibited, or the receptor itself is blocked from binding (Golshani & Zhang, 2020). Doing so prevents the continuation of the cell cycle, by downregulating the RAS-RAF-MEK-ERK pathway (Kumar et al., 2023).

Three of the most commonly utilised immunotherapies are anti-programmed cell death protein-1 (PD-1), anti-programmed death-ligand 1 (PD-L1), and anti-cytotoxic T-lymphocyte associated-antigen 4 (CTLA-4), these antibodies work towards preventing binding events for immune checkpoints. The binding interactions would normally result in T-regs forming as opposed to anti-tumour effectors (Figure 6). However, the use of these immune checkpoint inhibitors maintains the presence of activated effector T-cells, promoting the killing of tumour cells (Kumar et al., 2023).

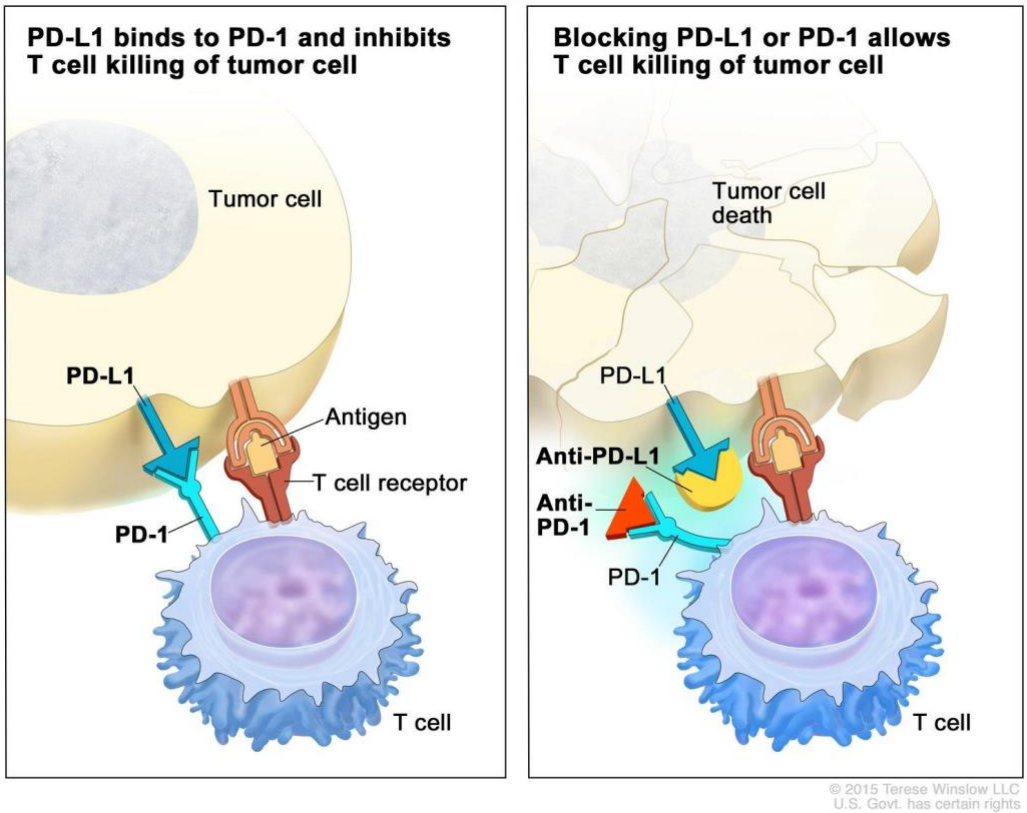

Figure 6. Immune checkpoint inhibitors prevent PD-L1 and PD-1 binding which allows for T-cell activation and death of the tumour cell (National Cancer Institute, 2022).

Finally, adoptive cell therapy utilises the patient's own T-cells to personalise the treatment. This process involves extracting the T-cells that have already been produced in the body and modifying them in vitro to increase their efficacy through genetic engineering techniques (Rosenberg & Restifo, 2015). This approach has shown success in many studies, but the personal nature of the treatment makes it significantly more expensive, limiting accessibility (Golshani & Zhang, 2020).

The most effective immunotherapy approach for CRC is still unclear, this review focuses on SOCS3 and IDO, components of the janus kinase and signal transducer and activator of transcription (JAK-STAT) signalling pathway.

1.5. JAK-STAT Signalling Pathway

Suppressors of Cytokine Signalling (SOCS) proteins are involved in negatively regulating the production of cytokines through the JAK-STAT signalling pathway. The production of these cytokines plays a number of important roles in cell mechanisms including differentiation, proliferation, maturation, and apoptosis (Inagaki-Ohara et al., 2013). Specifically, the JAK-STAT pathway allows signals from cytokines, interleukins (ILs), and growth factors to be transferred from cell membranes through binding to receptors, to the nucleus, which in turn allows responses to be generated (Figure 7) (Seif et al., 2017). Cytokines can either be pro-inflammatory, or anti-inflammatory, and these are released from cells in response to environmental changes, for example during infection (Carow & Rottenberg, 2014). Following the binding of the cytokine to type I and type II cytokine receptors, the receptors associate with JAKs. There are four JAKs present in mammals, these are JAK1-3 and TYK2, and upon binding to the receptor, they are phosphorylated (Carow & Rottenberg, 2014). These activated JAKs then phosphorylate the tyrosine residues of receptor cytoplasmic tails (Carow & Rottenberg, 2014). STATs can then bind to these phosphorylated regions via their SH2 domains which causes them to be phosphorylated via JAKs, undergo a confirmational change and release from the receptor (Gutierrez-Hoya & Soto-Cruz, 2020). This phosphorylated STAT can then bind to another phosphorylated STAT becoming a homodimer before translocating to the nucleus and binding to target genes promoting transcription (Gutierrez-Hoya & Soto-Cruz, 2020).

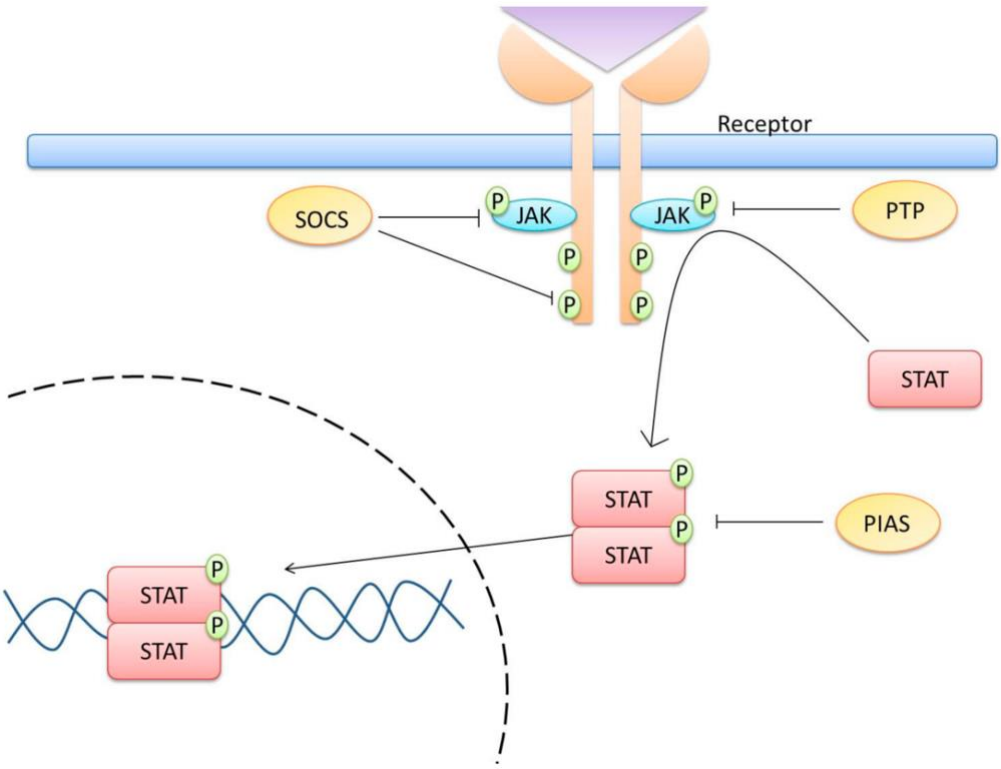

Figure 7. JAK-STAT signalling pathway upon cytokine binding (sourced from Gutierrez-Hoya & Soto-Cruz, 2020).

Negative regulation of the JAK-STAT signalling pathway can occur through protein tyrosine phosphates (PTP), protein inhibitors of activated STATs (PIAS) and SOCS proteins (1-7) which prevent JAK-STAT activity by competing with STAT, promoting degradation via ubiquitination and by acting as kinase inhibitors of JAK proteins (Carow & Rottenberg, 2014; Rico-Bautista et al., 2006).

1.6. Suppressor of Cytokine Signalling (SOCS) Proteins

SOCS proteins are part of a family of eight proteins (SOCS1-7 and cytokine-inducible SRC homology 2 (SH2)-domain-containing proteins (CIS)) involved in the regulation of cytokine signalling pathways (Yoshimura et al., 2007). These proteins each have a central SH2 domain which is thought to be what determines the protein's target, an amino N-terminal domain which is variable in length and a carboxyl-terminal known as the SOCS box (Yoshimura et al., 2007) (Figure 8). SOCS1 and SOCS3 have a small additional region within the N-terminal known as the kinase inhibitory region (KIR) which is what enables the protein to directly

inhibit JAK tyrosine kinase activity by preventing the phosphorylation of STAT1 (Rico-Bautista et al., 2006; Yoshimura et al., 2007).

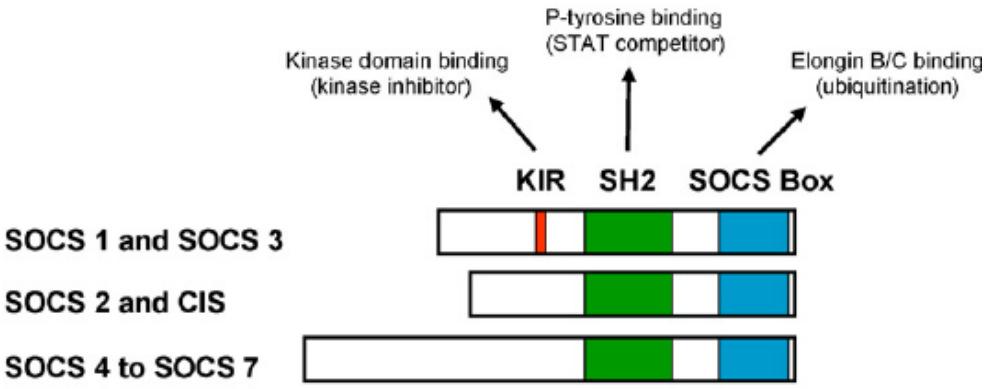

Figure 8. General structures of SOCS family proteins (sourced from Rico-Bautista et al., 2006).

The importance of these proteins has been shown through gene deletion studies in mice, for example, SOCS1 knockout (k/o) mice die within a few weeks of birth and SOCS3 knockout mice are not viable due to placental abnormalities (Alexander & Hilton, 2004).

There is growing evidence that SOCS proteins are linked to certain diseases, one of which is cancer.

1.7. Suppressor of Cytokine Signalling 3 (SOCS3)

SOCS3 prevents signal transducer and activator of transcription 3 (STAT3) activation by directly binding to the JAK kinase and the glycoprotein 130 kDa (gp130) cytokine receptor simultaneously (Carow & Rottenberg, 2014). The gp130 receptor is a type 1 cytokine membrane-bound receptor which interacts with cytokines from the IL-6 family and results in the activation of STAT3 through the JAK-STAT pathway (Kang et al., 2019; Rose-John, 2018). Gene deletion studies have shown that gp130 plays an essential role in embryogenesis and in regulating inflammation (Schmidt-Arras et al., 2014; Yoshida et al., 1996). Cytokines within the IL-6 family include IL-6, IL-11, and IL-27, and these all dimerise gp130 and result in

the expression of genes involved in proliferation, immune regulation, and differentiation (Rose-John, 2018).

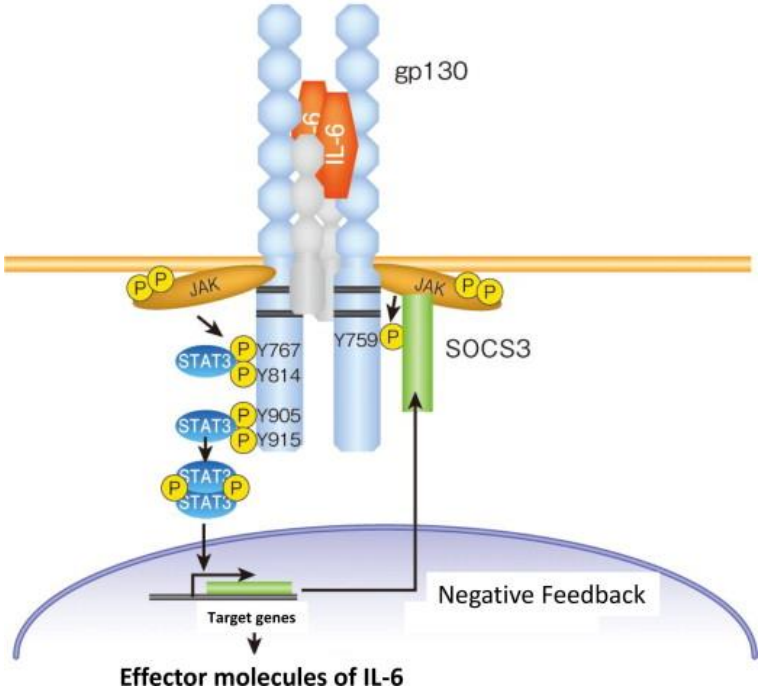

Figure 9. Activation of the JAK-STAT signalling pathway following IL-6 binding, a negative feedback loop is produced via SOCS3 binding to gp130 (Murakami et al., 2014).

IL-6 is an important inflammatory cytokine produced in response to infection and it results in the transcription of multiple pathways upon binding to gp130 (Tanaka et al., 2014). It is one of the major cytokines found within the tumour microenvironment due to its pro-inflammatory nature and its ability to regulate apoptosis, proliferation, and angiogenesis when uncontrolled (Kumari et al., 2016; Schneider et al., 2000). SOCS3 is a negative regulator of the JAK-STAT pathway, therefore when it directly binds to JAK and the gp130 receptor, STAT phosphorylation is prevented, and target genes are not produced. Another way in which SOCS3 regulates signalling is through a signalling cascade which results in the ubiquitination of signalling components via the E3 ubiquitin ligase complex, however, it does this with lower affinity compared to direct binding to JAK (Kershaw et al., 2014).

Many studies have shown that SOCS3 is integral to regulating inflammation and infection. The reduction or deletion of SOCS3, observed in a number of CRC tumours, was found to result in continuous activation of STAT3 (Dai et al., 2021; Carow & Rottenberg, 2014). The

silencing of SOCS3, found in multiple tumour types through hypermethylation of DNA (Neuwirt et al., 2007) warrants its recognition as a tumour suppressor.

Although the most widely researched tumour-suppressive role of SOCS3 is as a regulator of the JAK/STAT pathway, there is evidence of additional mechanisms. SOCS3 has been found to degrade CD33, a member of the sialic acid-binding immunoglobulin-like lectin family that has been found to be overexpressed in acute myeloid leukaemia (Carow & Rottenberg, 2014; Suwannasom et al., 2019). Furthermore, Emanuelli et al. (2000) demonstrated that SOCS3 expression was induced by insulin via STAT5B in order to inhibit activation, thereby regulating insulin sensitivity. The interactions of SOCS3 in different infections makes it difficult to determine its primary role, as it shows a tendency to stimulate multiple pathways in response to viruses, parasites, and bacteria (Carow & Rottenberg, 2014). SOCS3 has been shown to prevent immune tolerance by forming a complex with the enzyme indoleamine 2,3-dioxygenase (IDO) and promoting its degradation (Carow & Rottenberg, 2014).

1.8. IDO

Indoleamine 2,3-dioxygenase (IDO) is a rate-limiting enzyme involved in catalysing the catabolism of the essential amino acid tryptophan (TRP) into kynurenine (KYN) (Figure 10) (Mbongue et al., 2015). There are two types of IDO, IDO1 and IDO2, both of which catalyse the breakdown of TRP but IDO1 at a greater rate (Bilir & Sarisozen, 2017). IDO expression has been previously noted in endothelial, epithelial, mature DCs and macrophages (Bilir & Sarisozen, 2017; Zhai et al., 2020).

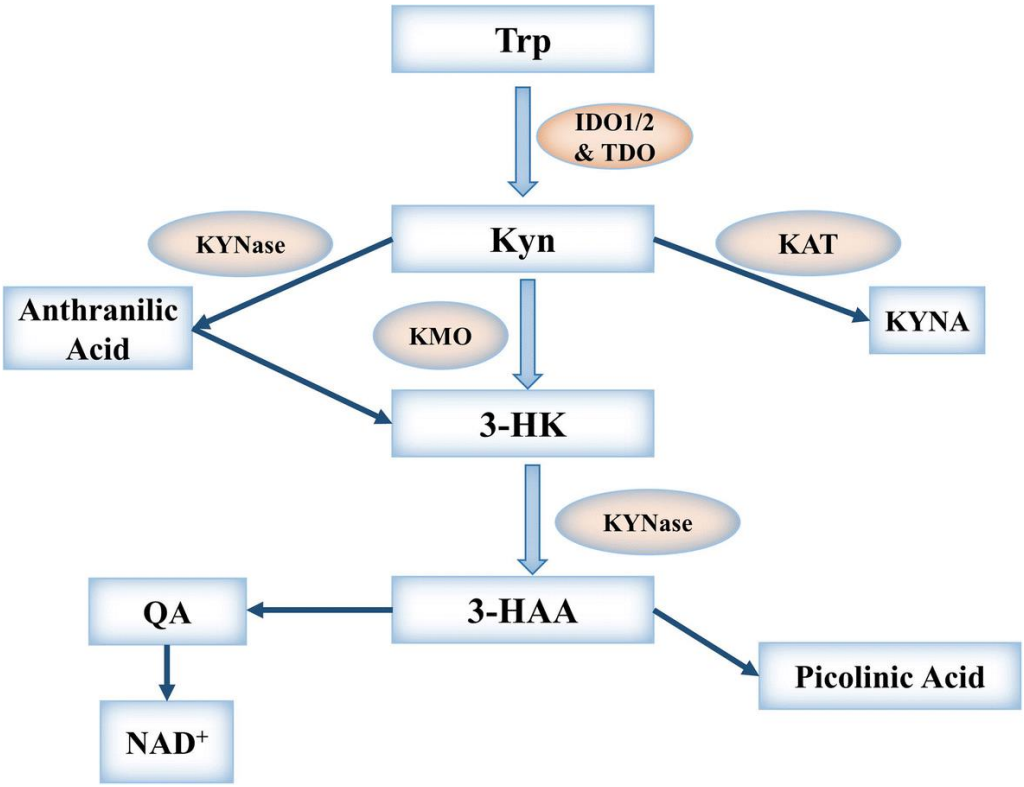

Figure 10. Tryptophan Metabolism Pathway (Liu et al., 2018).

IDO is produced in response to pro-inflammatory cytokines such as IFN-γ during periods of infection and has been associated with immune tolerance as it has been found at higher levels in the tumour microenvironment (Liu et al., 2018; Mellor & Munn, 1999). The mechanism by which this occurs is thought to be through the creation of a TRP-starved state in cells, causing T-cells to undergo cell cycle arrest preventing differentiation into effector T-cells (Wang et al., 2020). Additionally, KYN, the metabolite of TRP, has been found to be an immunosuppressive catabolite, which itself prevents the formation of effector T-cells that are able to fight cancerous cells (Routy et al., 2016).

IDO is overexpressed in many cancers including colorectal, melanoma and lung, and high expression is correlated with poor prognosis and survival rates (Bilir & Sarisozen, 2017; National Cancer Institute, 2023). IDO was also found to be expressed by DCs and macrophages, important antigen-presenting cells involved in cancer immunity, which could suggest increased IDO has the potential to induce tolerance via these immune cells to cancerous tumours (Munn et al., 2004; Vacchelli et al., 2014). Jiang et al. (2020) found that

the recruitment of macrophages and phagocytosis was inhibited by IDO in *Aspergillus fumigatus* via the MAPK/ERK-dependent pathway, presenting IDO's involvement in the polarisation of M1 macrophages. This supports the conclusion that the presence of M1 macrophages could indicate the success of immunotherapies through the administration of IDO inhibitors. However, this study used a fungal model and the effect IDO has on the human immune system may differ due to differing cellular structures, physiologies, and genetics (Jiang et al, 2020). Furthermore, Shaw et al. (2017) found that a loss of SOCS3 decreased resistance to helminth infection and this was associated with increased IDO.

Clinical trials reviewed by Fujiwara et al. (2022) showed promise when treating patients who have advanced malignancies with IDO inhibitors, as the immunosuppressive effects of the tumours were reduced. Despite this, there were many instances where the patients did not show a response. The review concluded that associated pathways may provide an explanation why the treatment had contradicting effects, referencing the need to optimise the efficacy of this immunotherapy.

1.9. SOCS3/ IDO Cancer Survival Axis

Normally, IDO is regulated via SOCS3 through direct binding which occurs when there is IL-6 present during periods of infection, allowing for CD28 binding to occur and T-cells to become effectors (Orabona et al., 2008). When these effector T-cells are no longer required, CTLA-4 binding occurs with higher affinity, which causes the cells to become regulatory (Orabona et al., 2008) (Figure 11). However, in the absence of SOCS3, IDO levels increase and reduce the amount of available tryptophan (Orabona et al., 2008). Subsequently, CD28 becomes immunosuppressive as T-cells cannot differentiate without tryptophan (Lee et al., 2002). This is considered to mimic the promotion of T-regulatory cells observed when CTLA-4 binds in the SOCS3-regulated environment (Orabona et al., 2008). Therefore, the dysregulation of IDO has been heavily associated with tumour development as it enables an immune tolerance.

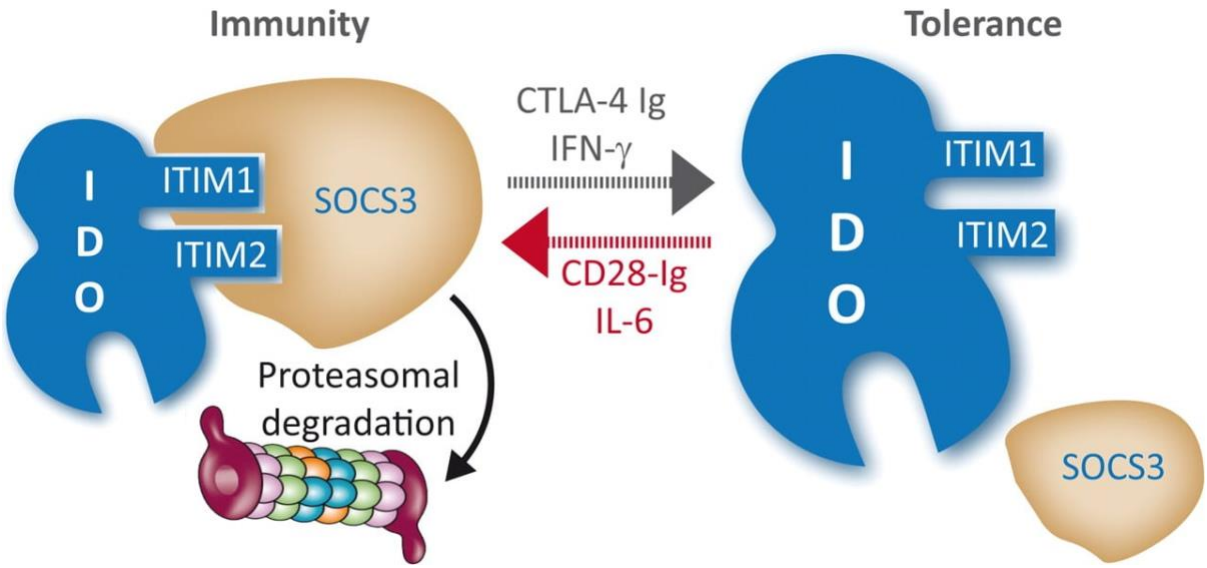

Figure 11. IDO/SOCS3 negative feedback loop (Orabona et al., 2008).

There have been many studies highlighting the importance of SOCS3 in regulating tumour development in cancer. Rigby et al. (2007) found that overexpression of SOCS3 in mice reduced the proliferation of cells through inhibition of the JAK-STAT signalling pathway, suggesting that the SOCS3 expression is an important modulator in promoting immune tolerance. However, overexpression of SOCS3 has been found in mice with chronic inflammation in the intestine, highlighting the importance of the balance of this regulatory protein (Rigby et al., 2007).

1.10. IDO Inhibitors

Due to the immune tolerant effects elevated IDO exhibits in cancer, many researchers have focussed their attention on developing IDO inhibitors as a potential treatment for cancer. Many of these IDO inhibitors, such as Epacadostat and Indoximod, are currently undergoing trials (Tang et al., 2021). In vitro, Epacadostat was found to increase NK cell and T-cell proliferation, as well as suppression of T-regs and in animal models it suppressed tumour growth in immunocompetent mice, but not immunodeficient mice (Jochems et al., 2016). This inhibitor has been trialled in combination with immune checkpoint inhibitor Pembrolizumab in a large phase three trial. However, little efficacy success was seen with no improvement in overall survival (Mitchell et al., 2018). Indoximod is another IDO

inhibitor under investigation, and success has been identified through its ability to reduce the suppression of T-cell proliferation, however, it was unable to arrest tumour growth (Günther et al., 2019). The current research implies tailored treatment may be necessary to achieve effective IDO inhibitor therapy, which could see greater efficacy if genotype screening of patients was completed upon diagnosis. Doing so, with knowledge as to the effects specific immune markers have on related immunotherapies, could greatly reduce the expense of treatment on the NHS. While enabling treatments with greater success rates to become accessible as time and resources are not used where they are likely to fail.

Current unpublished research by Whittingham-Dowd et al. (in preparation, 2024) identified the significance of SOCS3 within the STAT3 signalling pathway and how this could be a factor which contributes to immunotherapy resistance. Using IECS3 -/- mice which have undergone AOM/DSS treatment, 1-methyl-D-tryptophan (1-MT), an IDO blocker currently under research, was unable to reduce tumour burden in mice where SOCS3 was silenced compared to those without SOCS3 silencing. Additionally, IDO expression was found to be greater in the mice which lacked intestinal epithelial cell (IEC) SOCS3. These findings could indicate those with natural silencing of SOCS3 through hypermethylation in tumours, could hinder IDO inhibitor therapy.

1.11. Project Aims and Objectives

CRC is the second most common type of cancer, and currently, there is a lack of effective treatments available. Immunotherapy is a developing field in cancer research, the ability to personalise immunotherapeutic treatments presents a pathway to kill cancer cells with greater efficacy on a patient-by-patient basis. However, current approaches can be costly, with a significant risk of side effects. Hence, finding a suitable approach for each case could greatly improve the course of a patient's treatment.

Previous research has shown that IDO blockers have been successful in murine models, but when applied to humans, have presented variable results. Expression of SOCS3, an IDO mediator, has been identified as a potential contributor to the success rate of IDO blocker

therapy. Therefore, this project aims to investigate the effects of IDO inhibitors in SOCS3 sufficient and knockout tumours in a murine model of colon cancer.

Specific Aims:

Aim 1) To establish whether SOCS3 modulates the tumour immune environment, with particular regard to macrophage phenotype, in a murine model of CRC.

Aim 2) To establish whether IDO is more active in SOCS3 deficient tumours and thus contributes to an immunosuppressive tumour environment in vivo.

Aim 3) To investigate whether IDO inhibitors directly influence macrophage polarisation in vitro.

2. Materials and Methods

2.1. Animal Model

Following the institutional ethical approval, all experiments were conducted in accordance with Lancaster University physiological services unit regulations for animal husbandry, ethical guidelines and under Home Officing licencing in accordance with the Animals in Science Procedures Act (1986); PPL:415-7153.

Mice homozygous for pLox sites surrounding the gene coding for SOCS3 from C57BL/6 background (Croker et al., 2003) were crossed with hemizygous villin cre (VC) homozygous floxed SOCS3 from C57BL/6 background (Jackson Labs, Bar Harbor, ME, USA) to produce SOCS3 IEC knockout mice (housed at Lancaster University).

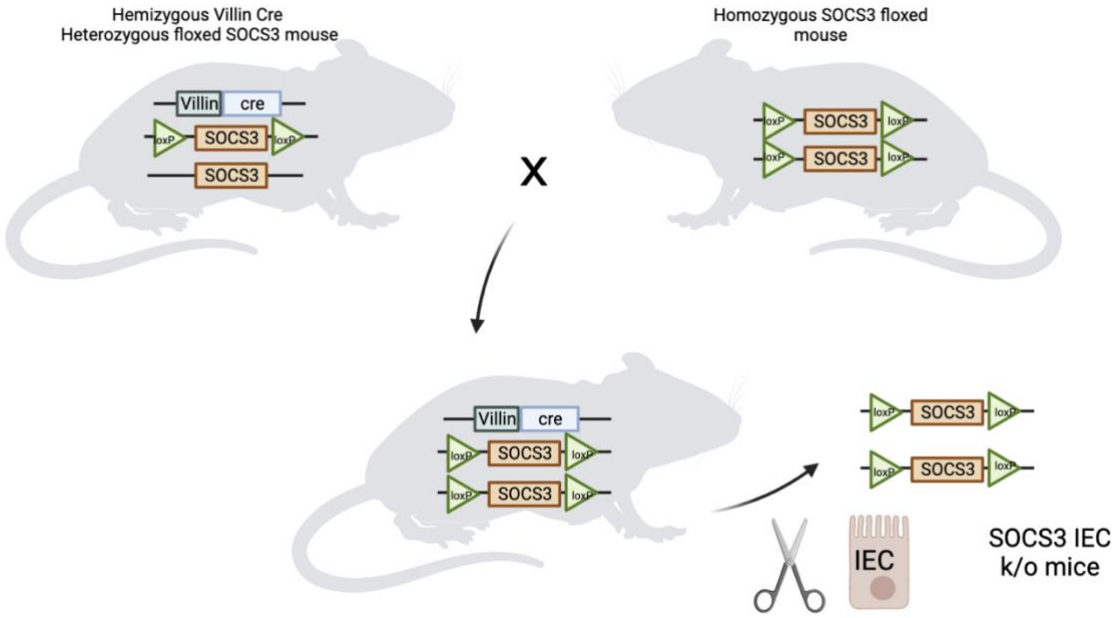

Figure 12. Schematic to show the method of producing IECS3 -/- mice (figure produced using BioRender.com).

Six- to 8-week-old, sex-matched IECS3 -/- and wildtype (wt) homozygous SOCS3 floxed littermates were treated with a single intraperitoneal injection of 10 mg/kg azoxymethane (AOM) (Merck, A5486). They were then administered 2.5% dextran sodium sulphate (DSS) (MPbio, 0216011025) which was alternated with 1-MT (Sigma, 860646-1G) (1 mg/mL) or

water treatment as shown in Figure 13. The mice were humanely killed 100-120 days following initial AOM treatment.

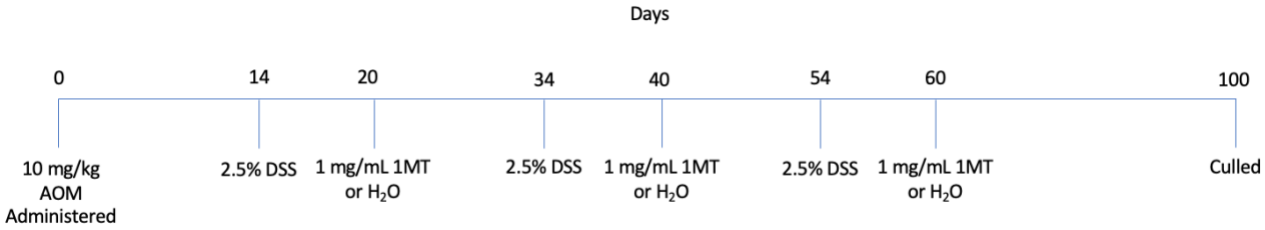

Figure 13. Timeline of SOCS3 IEC knockout mice treatment. *Treatment was started when mice were 6-8 weeks old (day 0).*

2.1.1. Genotyping

To confirm whether the mice were homozygous or heterozygous for the pLox sites, VC transgene or floxed/ cre excised alleles, ear snips were digested in 200 µL genotyping buffer (Appendix 1) with 6 µL 10 mg/ mL proteinase K (Sigma, P2308) overnight at 55°C, increasing to 95°C for 10 minutes before being put onto ice. Genotyping was carried out on 1 µL of the digested tissue using 10 µL 2x DreamTaq green PCR master mix (Thermofisher, K1081), 1 µL 10 µM forward and reverse primers (Table 1), and 7 µL sterile water (H_2O). Polymerase chain reaction (PCR) conditions of 1 minute at 95°C, then thirty-four cycles of 30 seconds at 95°C, 30 seconds at 62°C , 1 minute at 72°C and 1 minute at 72°C. PCR product and a 100 bp DNA ladder (Invitrogen, 15628-050) were run on a 1% agarose gel (Sigma, A9539) containing 5.6 µL safe view nucleic acid stain (NBS Biologicals, NBS-SV1) in tris-borate-EDTA (TBE) buffer (Appendix 1) for 30 minutes at 100 V. The gel was imaged using the iBright FL1500 (Thermofisher).

Table 1. Primers used to genotype mice. All were obtained from Sigma.

Primer (F/R)	Forward	Reverse
WT or SOCS3 floxed alleles	5'-GAGTTTTCTCTGGGCGTCCTCCTA-3'	5'-TGGTACTCGCTTTTGGAGCTGAA-3'
VC Transgene	5'-CTGCCACGACCAAGTGACAGC-3'	5'-CTTCTGTAGACCTGCGGTGCT-3'

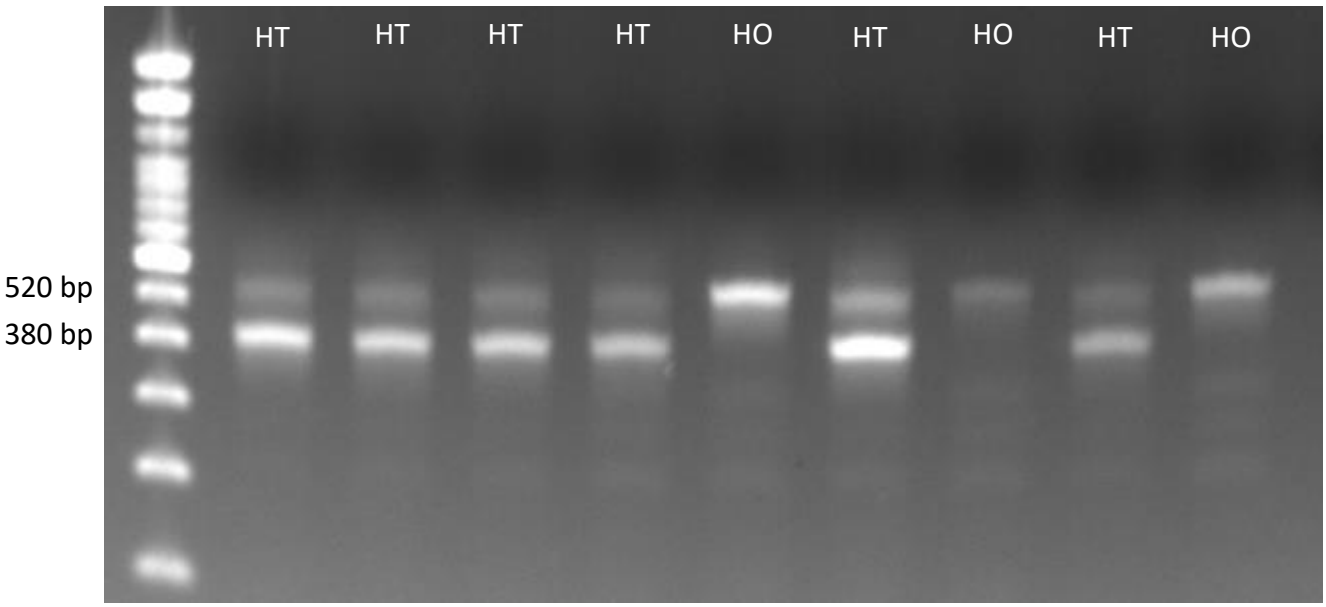

Figure 14. Genotyping of mice to determine whether they are heterozygous (HT) or homozygous (HO) for floxed SOCS3 alleles. WT= ~380bp, HO= ~520bp. *Ear snips were digested overnight at 55°C, incubated for 10 minutes at 95°C and put onto ice. Then 1 µL of each DNA sample underwent PCR before being run on a 1% agarose gel for 25 minutes which was imaged using the iBright FL1500. The first band at ~520bp indicated homozygous (HO) floxed SOCS3 alleles, second band at ~380bp indicated wildtype SOCS3 allele.*

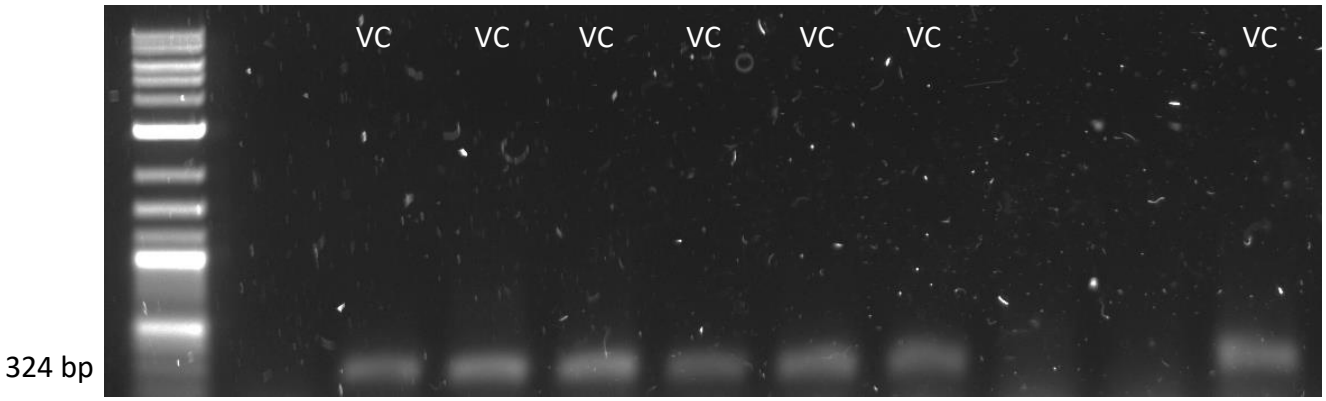

Figure 15. Genotyping of mice to determine whether they have the villin cre transgene (VC). VC= ~324bp. *Ear snips were digested overnight at 55°C, incubated for 10 minutes at 95°C and put onto ice. The 1 µL of each DNA sample underwent PCR before being run on a 1% agarose gel for 25 minutes which was imaged using the iBright FL1500. A band at ~324bp indicated the presence of villin cre.*

2.2. High-Performance Liquid Chromatography (HPLC)

2.2.1. Preparation of Colon Tissue

WT and IECS3 -/- mice treated with 1-MT/ H_2O had their colon tissue (tumour and non-tumour regions) micro-dissected and stored at -80°C. Tissue was kept on dry ice and weighed. Tissue was homogenised in 1 mL cold Milli-Q water, using 1.4 mm zirconium oxide beads (Precellys, P000927-LYSK0-A) in a Hybaid Ribolyser (Thermo Fisher Scientific) set to a speed of 4 for 20 seconds. Samples were put onto ice to prevent degradation for 1 minute, this cycle was repeated for a total of 5 times. Following this, samples were centrifuged at 4°C, 15,000 rpm for 10 minutes using an Eppendorf centrifuge (Thermo Fisher Scientific). The supernatant was added to 3 mL chloroform and vortexed for 10 seconds. Samples were centrifuged at 4°C, 4,000 rpm for 10 minutes, using the Allegra X-15R centrifuge (Beckman Coulter), resulting in the production of three fractions, a pellet, lipid disk and aqueous supernatant. The aqueous supernatant was added to 3 mL HPLC acetonitrile (ACN), and samples were vortexed and incubated on ice for 30 minutes to allow for protein aggregation and precipitation. After incubation, samples were centrifuged again at 4°C, 4,000 rpm for 10 minutes. One mL supernatant was pipetted into three 1.5 mL protein low bind tubes per sample, each with five pierced holes in the lids completed using a sterile needle. Samples were frozen at -80°C for at least 3 hours before lyophilization.

2.2.2. Lyophilization Preparation

Frozen samples were collected and lyophilized under a vacuum for a period of 24 hours, at -76°C, 0.0010 mbar using the alpha 1-4 Christ freeze-dryer (Martin Christ). Samples were retrieved and stored at -80°C until HPLC analysis (see 2.2.3).

2.2.3. HPLC Analysis

Mobile phase (0.1% trifluoroacetic acid (TFA) in distilled water (dH_2O): Acetonitrile (90:10 v/v)) was made, filtered (Millipore Express Plus 0.22 µm filter) and degassed (Edwards). Freeze-dried samples were collected from -80°C, resuspended in 1 mL mobile phase and put

into amber 2 mL vials (Agilent Technologies, 5182-0716). A standard was made using 100 µg/mL of TRP, KYN, 3-hydroxyanthranilic acid (AA), kynurenic acid (KYNA), 3-hydroxyanthraniliac acid (3-HAA) and 3-hydroxykynurenine (3-HK) (all obtained from Sigma-Aldrich) with mobile phase and a blank using 1.5 mL mobile phase alone. An Agilent 1260 infinity II LC system was used to analyse the colon samples. Analysis was provided by an in-line degasser, a diode array detector (DAD), and a 2475 multiwavelength fluorescence detector (Agilent Technologies). Isocratic separations were on a TSK-Gel ODS-80 Ts (250 x 4.6mm 5 µL) column (Tosoh Bioscience LLC) with the mobile phase at a flow rate of 0.8 mL/min. Each sample was injected at 200 µL in triplicate and used to provide chromatographs in the UV-Vis spectra from 190 to 800 nm, in addition to having channels set to monitor for emissions of relevant metabolites on the fluorescence detector. TRP is detected at a wavelength of 297-348 nm, KYN, AA, 3-HK and 3-HAA are detected at a wavelength of 364-480 nm and KYNA is detected at a wavelength of 330-390 nm (Lesniak et al., 2013). For each analyte, limits of detection (LOD) and calibration curves were generated by injections of the standard and blank mobile phase into the HPLC and used for reference to their quantities in the colon tissue.

2.3. In Silico Analysis of M1/M2 Markers

Kaplan-Meier plots were generated to compare death rates for colon cancer based on the expression of inducible nitric oxide synthase (iNOS) and cluster of differentiation 206 (CD206) (M1 and M2 markers respectively). Plots showing the expression of gene mRNA for iNOS and CD206 against median overall survival for colon cancer were generated using Ambion microarray chips on KM Plotter (Lanczky & Gyorffy, 2021) which uses publicly available online cancer genome databases (https://kmplot.com/analysis/index.php?p=service). Data were analysed using JetSet probes and included data from 1302 patients for iNOS and CD206 expression in colon cancer. Upper quartile values were calculated when more than 50% of the patient cohort survived beyond the study length and survival values were generated. All the data were analysed using one-way analysis of variance (ANOVA) tests and t-tests using confidence limits of 95% (P-value <0.05*).

2.4. Immunohistochemistry General Method

2.4.1. Histology

WT and IECS3 -/- mice treated with 1-MT/ H_2O had their colon tissue fixed in 4% paraformaldehyde (PFA) as Swiss rolls and embedded in paraffin wax before being cut and put onto slides. To aid the adhesion of tissue, slides were coated in 1% acid alcohol [1% (v/v) concentrated hydrochloric acid (HCl), 70% ethanol (EtOH), and 29% H_2O] for 30 minutes, then rinsed in running water, immersed in dH_2O, and left to dry. Once dry, they were immersed in acetone for 10 minutes and then in [2%(v/v) 3-aminopropyltriethoxysilane (APES) (Sigma-Aldrich, A3648) in acetone] for 5 minutes. They were rinsed twice in dH_2O before being left to dry.

Paraffin-embedded tissue was cut into 7 µm sections (Leica). Cut sections were placed onto the surface of 40°C water in a bath allowing adhesion onto the APES treated microscope slides. Tissue-coated slides were left to dry overnight.

To check tissue orientation, slides were stained with Mayer's hematoxylin (Sigma-Aldrich, MHS16) and viewed using a bright-field microscope (Motic).

2.4.2. Deparaffinisation and Tissue Rehydration

Slides were deparaffinised and rehydrated using xylene and ethanol in the order presented in Table 2. After being washed in tris-buffered saline (TBS) for 5 minutes, they were kept in dH_2O until ready for antigen retrieval (see 2.4.3).

Table 2. Deparaffinisation and Tissue Rehydration Steps.

Xylene	Xylene	100% EtOH	100% EtOH	90% EtOH	70% EtOH	50% EtOH	1x TBS
5 min	5 min	3 min	1 min	1 min	1 min	1 min	5 min

2.4.3. Antigen Retrieval

Tissue-coated slides underwent heat-induced epitope retrieval using a water bath. Water was heated and maintained at 95˚C, slides were placed in a plastic slide container which was filled with tris-EDTA pH 9.0 buffer (Appendix 1) and placed in the water bath for 30 minutes. Following heating, slides were removed from the buffer and placed in TBS for 15 minutes.

2.4.4. Immunohistochemical Staining

2.4.4.1. Permeabilization and Blocking

Following antigen retrieval, slides were washed in TBS + 0.025% Triton X-100 (Appendix 1) for 5 minutes with gentle agitation and permeabilised in TBS + 0.25% Triton X-100 (Appendix 1) for 10 minutes with gentle agitation. Finally, they were washed with TBS + 0.025% Triton X-100 twice for 2 minutes.

Slides were blocked in 10% donkey normal serum (Sigma-Aldrich, D9663) in 3% bovine serum albumin (BSA) (Sigma, A3059) in TBS (Appendix 1) for 2 hours at room temperature.

2.4.4.2. Antibody Staining

After blocking, excess solution was removed from around the tissue and a 2 mm advanced PAP hydrophobic marker (Sigma-Aldrich, Z672548-1EA) was used to draw around the tissue. Recombinant rabbit monoclonal anti-ionized calcium binding adaptor molecule 1 (IBA-1) antibody against mouse (Abcam, ab178846) and polyclonal goat CD206 antibody against mouse (R&D Systems, AF2535-SP) were diluted to concentrations of 1:2000 and 1:100 respectively with 1% BSA in TBS (Appendix 1) and pipetted onto the tissue. Control tissue had normal rabbit immunoglobulin G (IgG) (Santa-Cruz Biotechnology, sc-2027) mixed with normal goat IgG (Santa-Cruz Biotechnology, sc-3887) both diluted to 1:800 in 1% BSA in TBS pipetted onto the tissue. Slides were left to incubate overnight at 4°C in a humidified chamber.

Following overnight incubation, slides were washed twice for 5 minutes in TBS + 0.025% Triton X-100 with gentle agitation. They had a final rinse with TBS for 10 seconds before the secondary antibody was added. Alexa Fluor (AF) 488 donkey anti-rabbit (Invitrogen, 21206) mixed with AF 594 donkey anti-goat (Santa Cruz Biotechnology, sc-362275) at concentrations of 1:200 and 1:100 (diluted in 1% BSA in TBS) respectively, were added to both the control and non-control tissue and incubated at room temperature in the dark for 1 hour.

Two 5-minute washes using TBS + 0.025% Triton X-100 with gentle agitation were completed and a final ten-second rinse with TBS. A drop of mountant with 4',6-diamidino-2-phenylindole (DAPI) (Fluoromount-G, Invitrogen, 00-4959-52) was added to the slides before they were coverslipped. Once dry, slides were stored in the dark at 4°C and imaged within 1 week of staining.

2.4.5. Data Analysis of Dual Stained Slides

Slides were imaged on the Zeiss LED axioscope equipped with an AxioCam ICm1 (0.5x), objective lens 20x, at a total magnification of 10x at a wavelength of 488 nm to image anti-IBA-1 staining of macrophages (artificially coloured green using Zen blue edition software 3.4), 594 nm to image CD206 staining of M2 macrophages (artificially coloured red using Zen blue edition software 3.4) and 358 nm to view DAPI staining of DNA (artificially coloured blue using Zen blue edition software 3.4).

Macrophage and CD206+ IBA1- cell counts were completed using ImageJ software, the average number present in a randomly placed 4 x 10^4 μm^2 box over non-tumour regions and the average present per mm^2 tumour tissue for each slide. These data were presented as scatter plots, with error bars representing the standard error of the mean (SEM).

All the data were analysed using a one-way ANOVA and a post hoc Tukey honestly significant difference (HSD) and Bonferroni's multiple comparison test using confidence limits of 95% (P-value <0.05*).

2.5. Cell Culture

2.5.1. Cell Maintenance

Human monocytic THP-1 cells (ECACC, 88081201) were maintained in culture in tissue flasks in Roswell Park Memorial Institute (RPMI) 1640 media with L-glutamine (Corning, 10-040-CV) + 10% fetal bovine serum (FBS) (Gibco, 11570506) at 37°C and 0.05% carbon dioxide (CO_2).

2.5.2. Cell Counts

Cells stored in a tissue flask were removed from the incubator and resuspended, 20 µL of cells were put into an eppendorf tube and mixed with 20 µL 0.4% (w/v) trypan blue in PBS (1:1 ratio) (Corning, 25-900-CI).

A haemocytometer was used to count the number of cells present under a light microscope (x40) (Motic, AE2000). The number of cells was counted in four grids and averaged, before being multiplied by 2 (dilution factor), and then by 10^4 giving the number of cells per mL. This was then multiplied by the total volume of cells to give the total number of cells in the suspension.

2.5.3. Polarisation of THP-1 Cells

THP-1 cells were seeded into chamber slide wells (Lab-Tek, 177402) at 100,000 cells/well and 24-well plates (Corning, 3526) at 500,000 cells/well and differentiated into macrophages by 24-hour incubation with 150 nM phorbol 12-myristate 13-acetate (PMA) (Merck, P1585), followed by 24 hours in RPMI media at 37°C and 0.05% CO_2.

M1 macrophage polarisation was completed by cytokine stimulation with 20 ng/mL IFN-γ (PeproTech, 300-02) and 10 pg/mL lipopolysaccharides (LPS) (Merck, L2630) in media for 24 hours, 37°C, 0.05% CO_2. M2 macrophage stimulation was completed by cytokine stimulation with 20 ng/mL IL-4 (PeproTech, 200-04) and 20 ng/mL IL-13 (PeproTech, 200-13) in media for 48 hours, 37°C, 0.05% CO_2. Control wells contained media alone. Experimental wells contained appropriate cytokines and 1 or 0.25 µg/mL 1-MT treatment.

Following polarisation, cells in chamber slides were fixed for labelling (see 2.5.4) and cells in 24-well plates were lysed for western blots (see 2.5.6).

2.5.4. Fixation, Permeabilization and Immunofluorescence Labelling

After 24/48 hours of treatment, cells in the chamber slides were fixed with cold 4% paraformaldehyde (Appendix 1) in phosphate-buffered saline (PBS) for 10 minutes before one 10-minute wash with 2% BSA in PBS (Appendix 1), one 10-minute wash with PBS + 0.25% Triton X-100 (Appendix 1) and one 10-minute wash with 2% BSA in PBS. Primary antibody, iNOS (Millipore, ABN26) (1:100, diluted with 2% BSA in PBS) for M1 macrophages or CD206 anti-mannose receptor rabbit polyclonal (Abcam, ab64693) (1:100, diluted with 2% BSA in PBS) for M2 macrophages was incubated on the appropriate slide overnight (control well was incubated in 2% BSA in PBS alone) at 4°C in a humidified chamber.

Cells were washed three times for 10 minutes with 2% BSA in PBS before incubation with AF 488 donkey anti-rabbit (Invitrogen, 21206) at a dilution of 1:1000 for 1 hour at room temperature. Cells were washed three times with PBS, mounted with DAPI (Fluoromount-G, Invitrogen, 00-4959-52) and coverslipped. Slides were stored in the dark at 4°C and imaged within 1 week of staining.

2.5.5. Data Analysis of Immunofluorescent Labelled Chamber Slides

Slides were imaged using the confocal microscope (Leica, Stellaris 5) at a magnification of 20x and 0.75 aperture. DAPI staining of DNA was imaged at an excitation wavelength of 405

nm (coloured blue) and iNOS/CD206 staining was imaged at an excitation wavelength of 499 nm (coloured green).

Cells with DAPI staining alone were counted using ImageJ software along with the number of DAPI-stained cells + iNOS/CD206 positively stained cells. The percentage of M1/M2 cells polarised was calculated for each treatment group. These were presented as bar charts +/- SD. All the data were analysed using a one-way ANOVA and a post hoc Tukey HSD and Bonferroni's multiple comparison test using confidence limits of 95% (P-value <0.05*).

2.5.6. Western Blots

After 24/48 hours of treatment, cells in the 24-well plates were washed with PBS before being lysed using fresh cell lysis buffer (Appendix 1), scraped and frozen.
Samples were mixed 3:1 with laemmli sample buffer (Bio-Rad, 161-0747) with β-mercaptoethanol and heated to 95°C for 5 minutes before being spun down and run on mini-protean TGX stain-free gels (Bio-Rad, 4568125) with 2.5 µL Precision Plus Protein Dual Colour Standards (Bio-Rad, 161-0374) as a ladder at 200 V for 30 minutes in laemmli sodium dodecyl sulphate-polyacrylamide gel electrophoresis (SDS-PAGE) running buffer (Appendix 1). The gel was activated for 1 minute and imaged on the Bio-Rad ChemiDoc MP imaging system to confirm the presence of protein before being transferred.

Protein was transferred to nitrocellulose membranes 0.45 µm (Bio-Rad, 1620145) equilibrated in transfer buffer (Appendix 1) at 25 V, 2.5 A for 7 minutes using the Trans-Blot Turbo Transfer System (Mixed MW programme, Bio-Rad). After transfer, the blot was blocked in 5% TBS-BSA for 1 hour at room temperature on the roller mixer (Stuart, SRT6). The membrane was transferred to a falcon tube containing IDO mouse monoclonal antibody (Santa-Cruz Biotechnology, sc-137012) at a concentration of 1:400 (diluted in 5% BSA in TBS (Appendix 1)) and incubated overnight at 4°C on the roller mixer.

The blots were washed three times with TBS + 0.01% Tween-20 (Appendix 1) for 10 minutes on the mini orbital shaker (Stuart, SSM1) and incubated with goat anti-mouse IgG-HRP (Santa-Cruz Biotechnology, sc-2031) at a concentration of 1:2000 (diluted in 5% BSA in TBS)

for 1 hour at room temperature on the roller mixer. A further six 5-minute washes were completed (with the final wash being in TBS alone) before they were developed using 1 mL Clarity Western ECL Substrate (Bio-Rad, 170-5056) for 5 minutes. Blots were imaged on the iBright FL1500 (Thermofisher).

A further 10-minute wash in TBS + 0.01% Tween-20 was carried out before the process was repeated with the next primary antibody (Table 3).

Table 3. Primary and secondary antibodies used (all diluted in 5% BSA in TBS).

Primary Antibody (Dilution)	Secondary Antibody (Dilution)
IDO mouse monoclonal antibody (Santa-Cruz Biotechnology, sc-137012) (1:400)	Goat anti-mouse IgG-HRP (Santa-Cruz Biotechnology, sc-2031) (1:2000)
SOCS3 rabbit antibody (Cell Signalling Technology, 2932S) (1:1000)	Chicken anti-rabbit IgG-HRP (Santa-Cruz Biotechnology, sc-516087) (1:2000)
α-tubulin mouse monoclonal IgM (Santa-Cruz Biotechnology, sc-8035) (1:200)	Goat anti-mouse IgG-HRP (Santa-Cruz Biotechnology, sc-2031) (1:2000)

2.5.7. Data Analysis of Western Blots

Blots were analysed using the iBright Analysis Software with each visible band having the volume (intensity) measured. Bands for SOCS3/ IDO were normalised using the loading control α-tubulin bands and the average for each treatment group was calculated. Each value was made relative to the media alone control group before being plotted as a bar chart +/- SD.

3. Results

3.1. Assessment of M1 and M2 macrophage markers and colon cancer survival

Kaplan-Meier plotter (Lanczky & Gyorffy, 2021) was used to generate data which allowed for comparison between the expression of gene mRNA for M1/ M2 macrophage markers and median colon cancer survival rates. Previous studies indicate M2 macrophages are thought to cause a pro-tumorigenic environment via tumour-promoting effects and immunosuppression, therefore you would expect high expression of M2 macrophages to be associated with worse survival rates.

3.1.1. M1 macrophage marker iNOS expression correlates to better median survival compared to lower expression in colorectal cancer cases

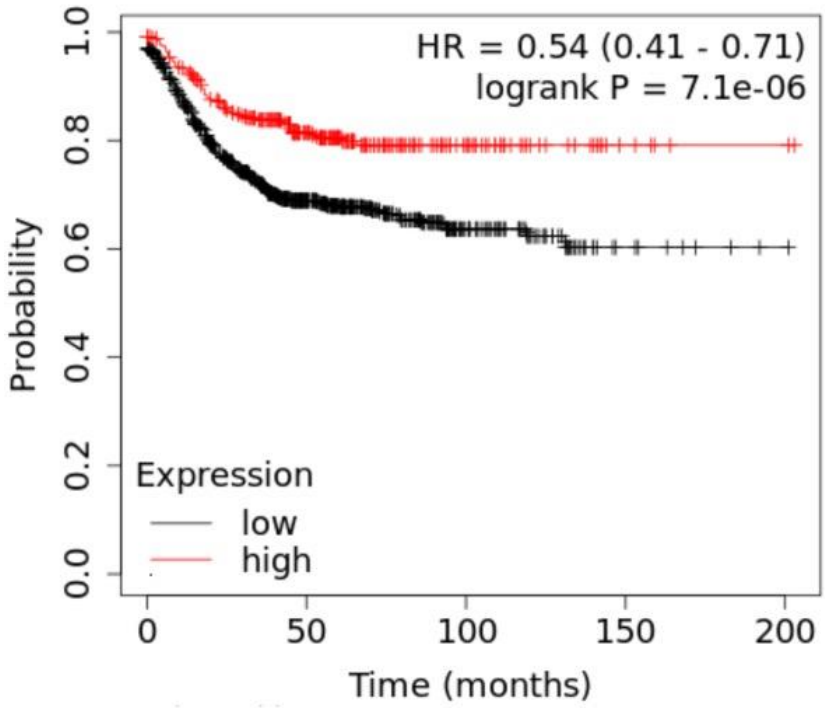

Figure 16. Probability of survival against time after diagnosis for high and low gene mRNA iNOS expression. *Publicly available online cancer genome databases were used to generate the data, and these were analysed using JetSet probes (n= 1302)***.** *HR = Hazard ratio. Data were analysed using a one-way ANOVA test and t-test using confidence limits of 95% (P-value= 7.1 x* 10^{-6}*).*

A significant difference was found between the expression of iNOS and the probability of survival over time, showing that a higher rate of gene mRNA iNOS expression is linked with a greater chance of survival over time than low expression. This could imply that a higher expression of M1 macrophages could improve survival in colon cancer.

3.1.2. M2 macrophage marker CD206 expression correlates to worse median survival in colorectal cancer cases

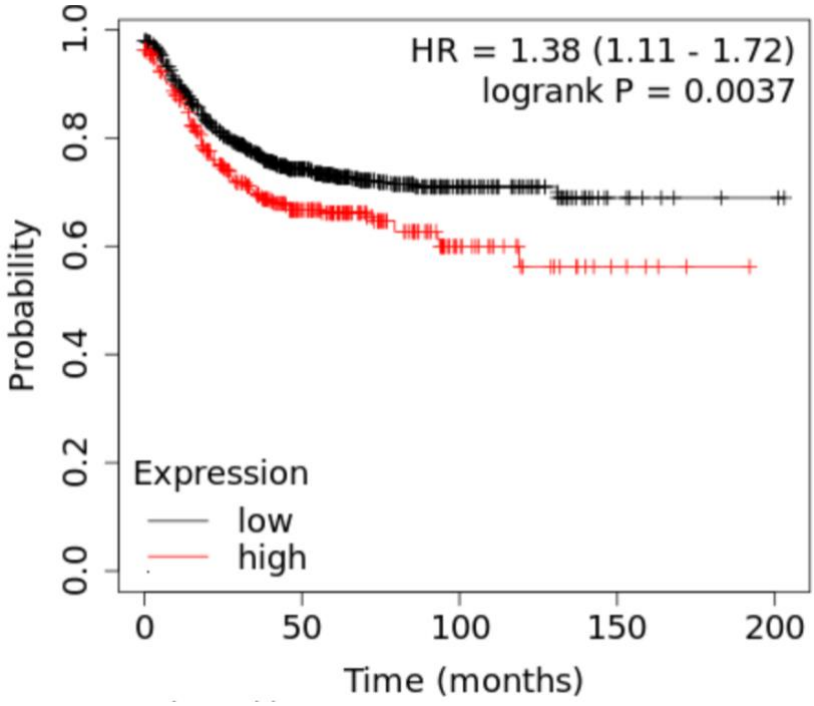

Figure 17. Probability of survival against time after diagnosis for high and low gene mRNA CD206 expression. *Publicly available online cancer genome databases were used to generate the data, and these were analysed using JetSet probes (n= 1302)**.** HR = Hazard ratio. Data were analysed using a one-way ANOVA test and t-test using confidence limits of 95% (P-value= 0.0037).*

A significant difference was found between the expression of CD206 and the probability of survival over time, showing that a lower rate of gene mRNA CD206 expression is linked with a greater chance of survival over time than high expression. This could imply that a high expression of M2 macrophages could reduce survival in colon cancer. This is in agreement with current literature, which suggests M2 macrophages are tumour-promoting and can be linked with immunosuppression (Pernot et al., 2014).

3.2. Assessment of M1 and M2 macrophage localisation and quantification in a murine model of colon cancer

To determine whether loss of epithelial SOCS3 or 1-MT treatment influences intra-tumoral or lamina propria recruitment of macrophages, dual labelling for tissue macrophages and M2 marker CD206 was performed in a murine model of CRC. IBA-1 was chosen as a general macrophage marker as it has proven to stain most macrophage subpopulations in both human and murine models, allowing for cross-species comparisons to be made. CD206 was chosen as an M2 macrophage marker as it is normally expressed on M2 macrophages but not M1 macrophages, it is also expressed by immature DCs (Xu et al., 2020). These antibodies were used to stain tumour and non-tumour regions of the colon in wildtype H_2O treated mice, wildtype 1-MT treated mice, IECS3 -/- H_2O treated mice, and IECS3 -/- 1-MT treated mice (Mikkelsen et al., 2017).

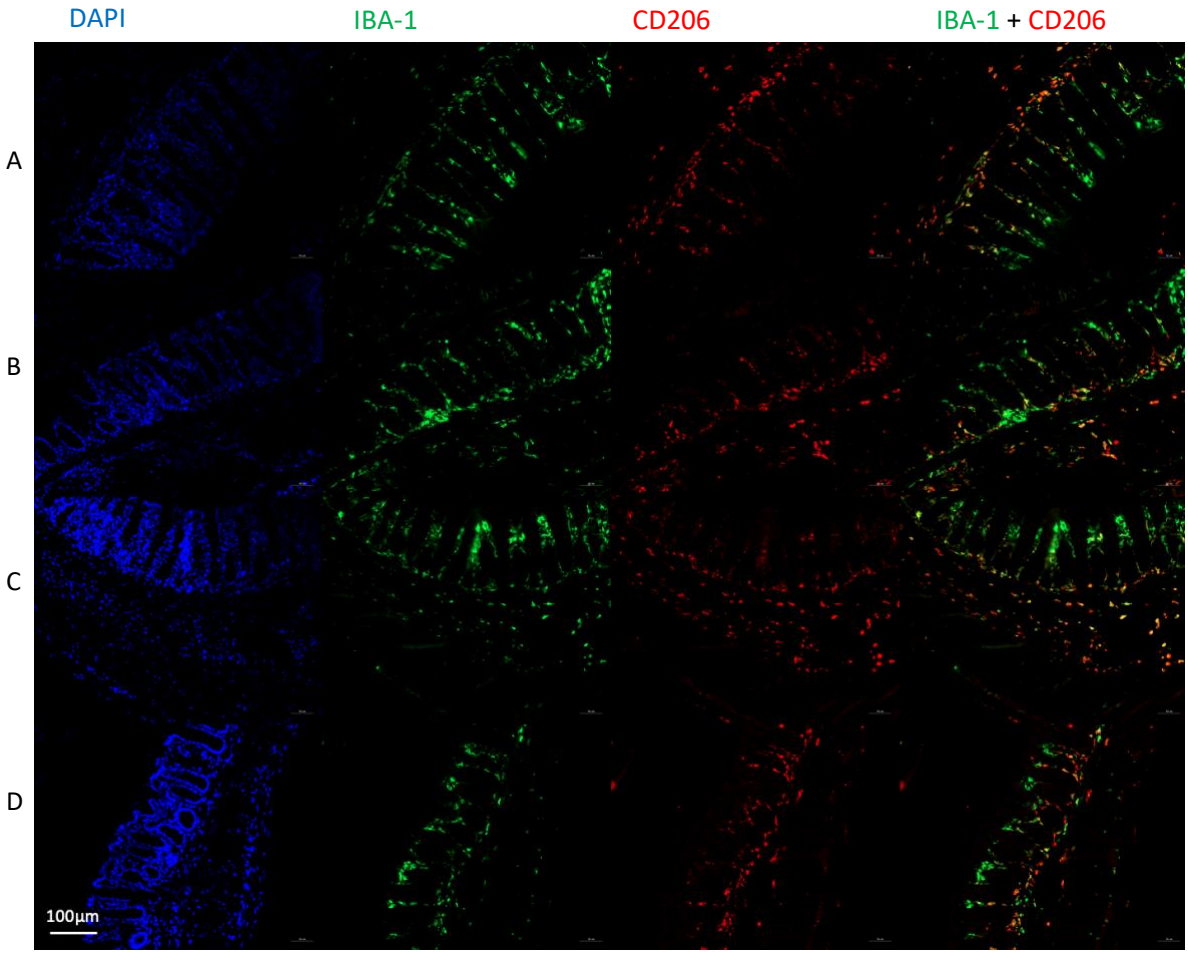

Figure 18. Immunohistochemistry of fixed paraffin-embedded sections of mouse colon non-tumour regions stained with anti-IBA-1 (ab178846) and CD206 (R&D Systems, AF2535-SP), A: WT H_2O, B: IECS3 -/- H_2O, C: WT 1-MT, D: IECS3 -/- 1-MT. *Tissue was imaged with the epifluorescent microscope (Zeiss LED) equipped with an AxioCam ICm1 (0.5x), total magnification of 10x, and coloured using ZEN blue 3.4 software. DAPI staining is shown in blue imaged at an excitation wavelength of 358 nm, IBA-1 staining is shown in green imaged at an excitation wavelength of 488 nm and CD206 staining is shown in red imaged at an excitation wavelength of 594 nm.*

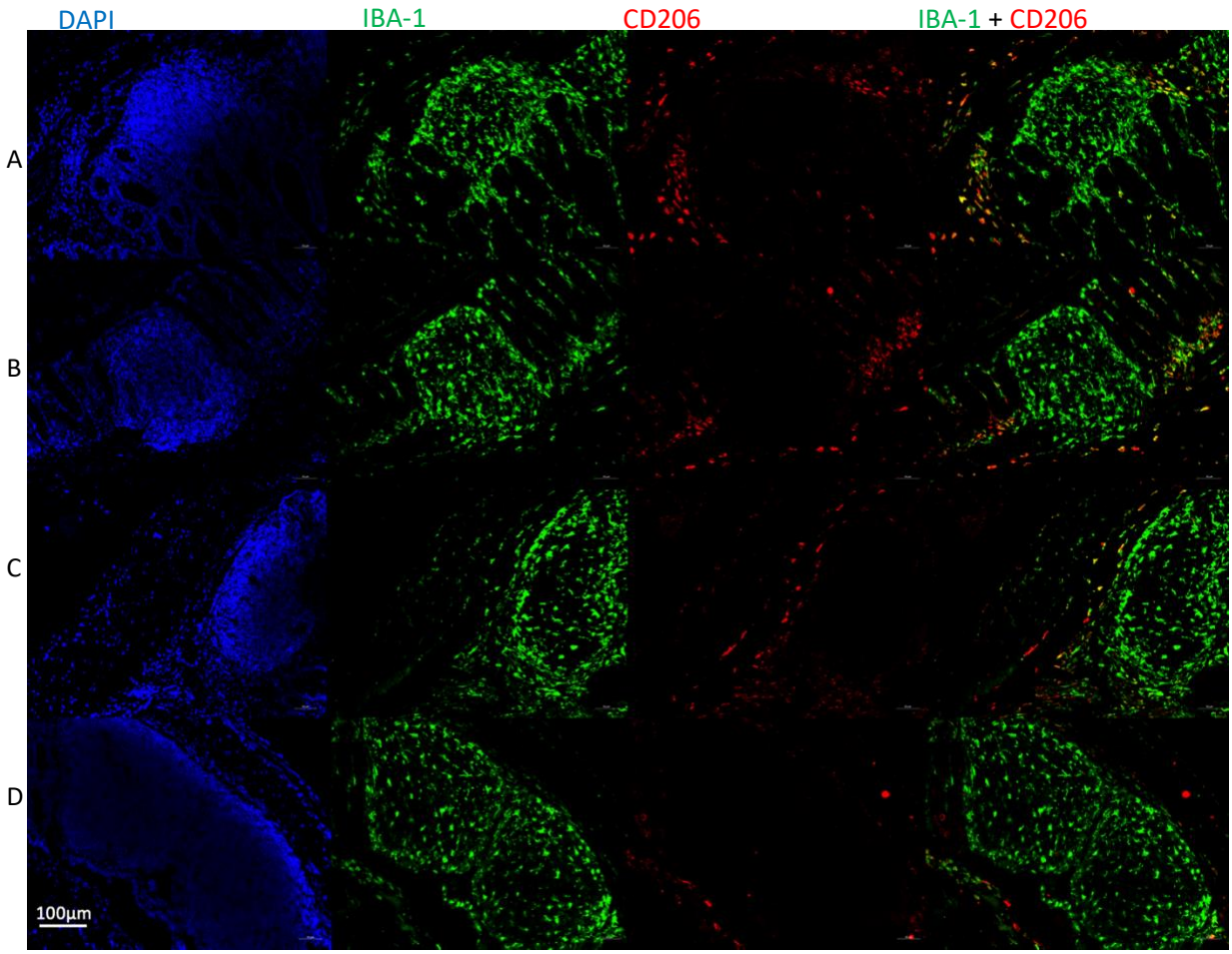

Figure 19. Immunohistochemistry of fixed paraffin-embedded sections of mouse colon tumour regions stained with anti-IBA-1 (ab178846) and CD206 (R&D Systems, AF2535-SP), A: WT H_2O, B: IECS3 -/- H_2O, C: WT 1-MT, D: IECS3 -/- 1-MT. *Tissue was imaged with the epifluorescent microscope (Zeiss LED) equipped with an AxioCam ICm1 (0.5x), total magnification of 10x, and coloured using ZEN blue 3.4 software. DAPI staining is shown in blue imaged at an excitation wavelength of 358 nm, IBA-1 staining is shown in green imaged*

at an excitation wavelength of 488 nm and CD206 staining is shown in red imaged at an excitation wavelength of 594 nm.

M1 macrophages are predominantly located in tumour regions as opposed to M2 macrophages in all four treatment groups. It also appears as though M2 macrophages tend to be localised in the laminar propria adjacent to the base of the crypts in non-tumour regions.

3.2.1. Loss of epithelial SOCS3 and/or 1-MT treatment does not affect the number of M1 macrophages found in non-tumour regions of the colon

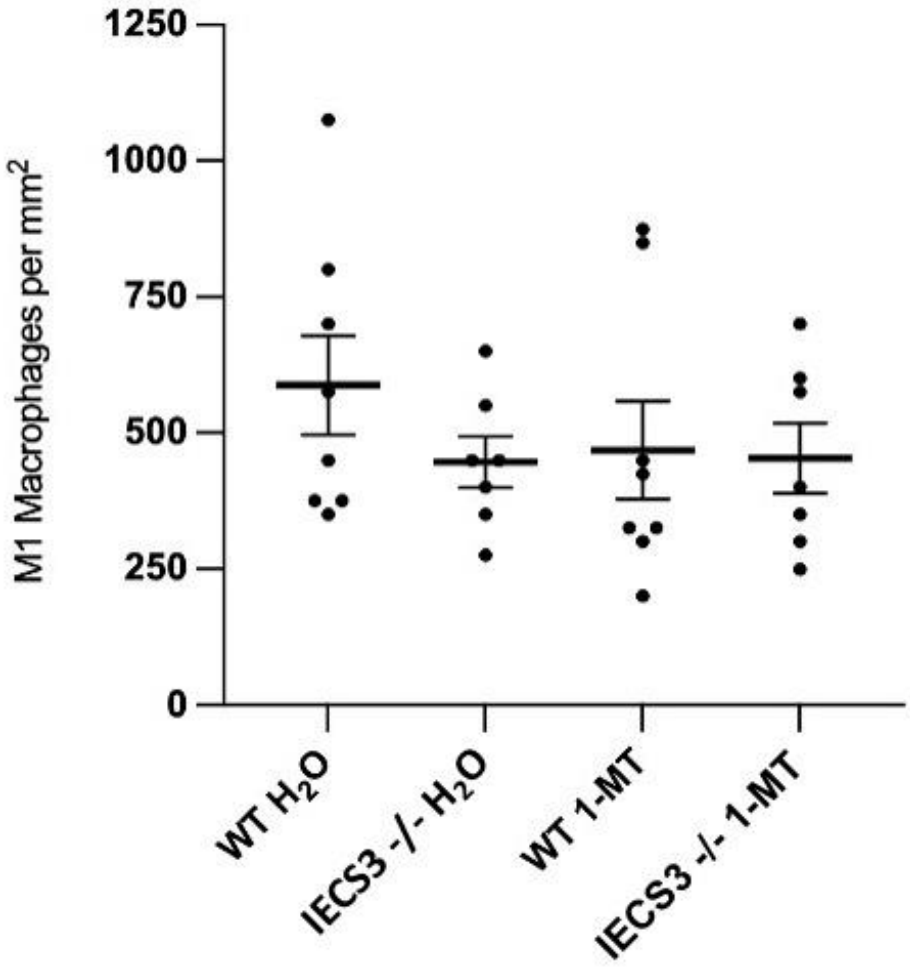

Figure 20. Average number of M1 macrophages per mm^2 non-tumour colon tissue in wildtype H_2O treated (n=6), wildtype 1-MT treated (n=7), IECS3 -/- H_2O treated (n=5), and IECS3 -/- 1-MT treated (n=5) mice. *Cell counts were carried out using ImageJ software, the*

average number of M1 macrophages was counted in a randomly placed 4 x 10^4 μm^2 box, and these data were presented +/- SEM. Data points in the plots represent data from one mouse. All the data were analysed using a post hoc Tukey HSD and Bonferroni's multiple comparison test using confidence limits of 95% (P=< 0.05).*

No significant difference was found between the number of M1 macrophages in non-tumour regions of the colon in the four treatment groups.

3.2.2. Loss of epithelial SOCS3 and/or 1-MT treatment does not affect the number of M2 macrophages found in non-tumour regions of the colon

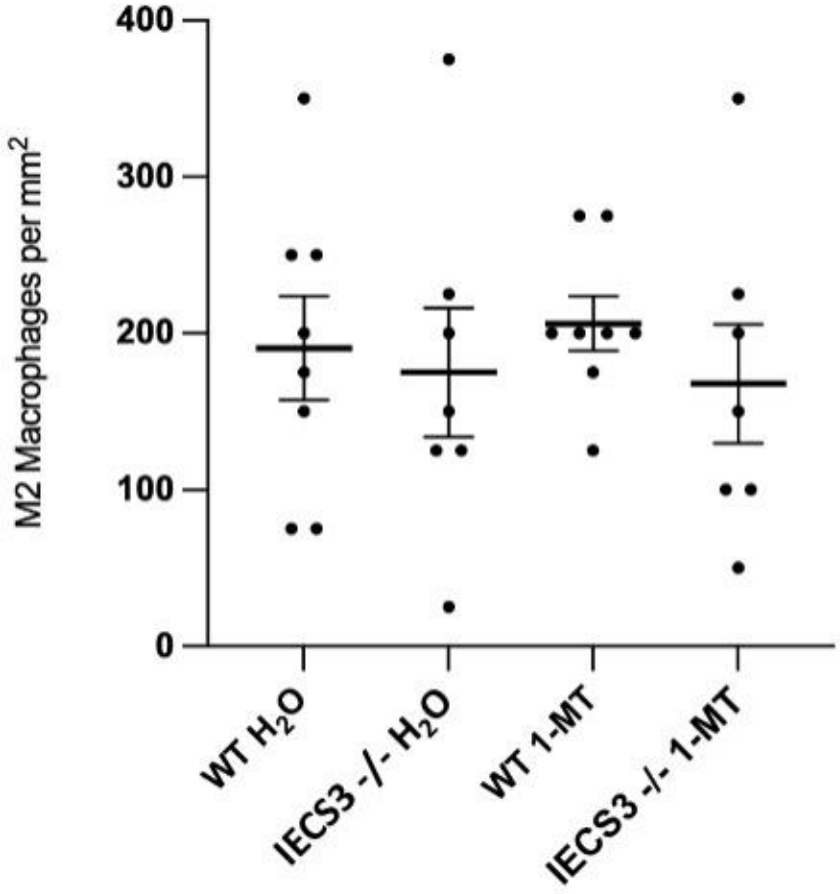

Figure 21. Average number of M2 macrophages per mm^2 non-tumour colon tissue in wildtype H_2O treated (n=6), wildtype 1-MT treated (n=7), IECS3 -/- H_2O treated (n=5), and IECS3 -/- 1-MT treated (n=5) mice. *Cell counts were carried out using ImageJ software, the average number of M2 macrophages was counted in a randomly placed 4 x 10^4 μm^2 box, and these data were presented +/- SEM. Data points in the plots represent data from one mouse.*

All the data were analysed using a post hoc Tukey HSD and Bonferroni's multiple comparison test using confidence limits of 95% (P=< 0.05).*

No significant difference was found between the number of M2 macrophages in non-tumour regions of the colon in the four treatment groups.

3.2.3. Loss of epithelial SOCS3 and/or 1-MT treatment does not affect the number of CD206+ IBA1- cells found in non-tumour regions of the colon

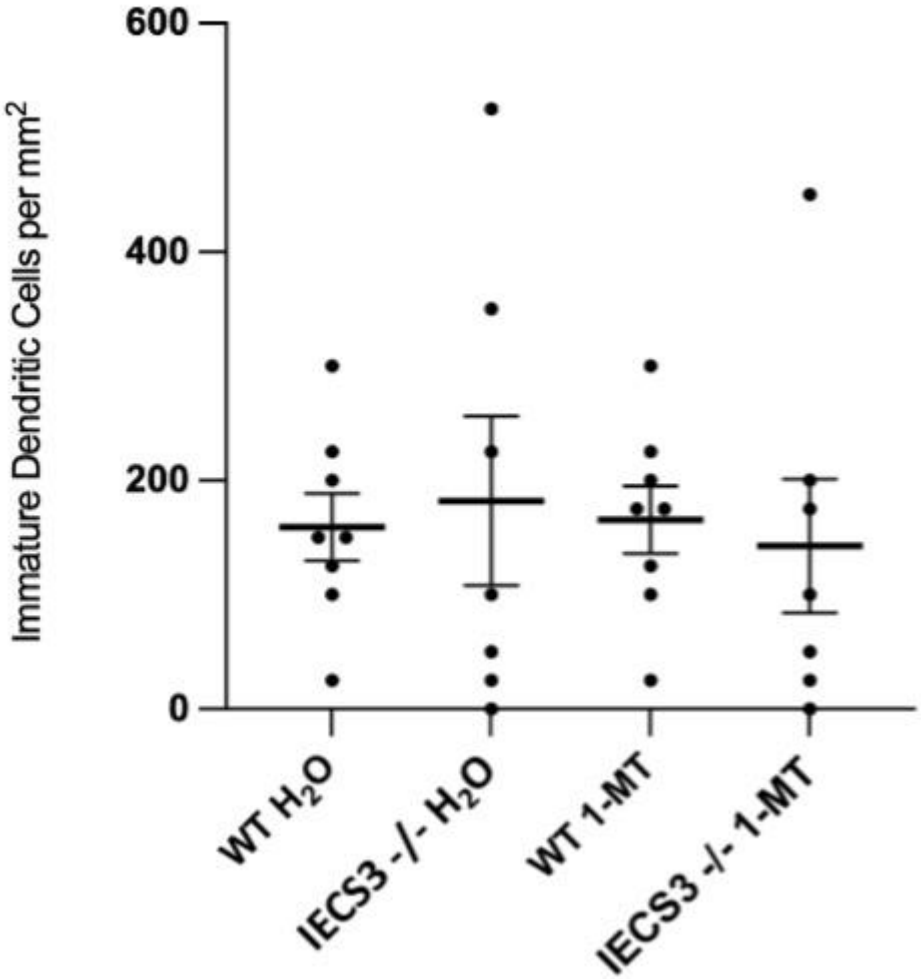

Figure 22. Average number of CD206+ IBA1- cells per mm^2 non-tumour colon tissue in wildtype H_2O treated (n=6), wildtype 1-MT treated (n=7), IECS3 -/- H_2O treated (n=5), and IECS3 -/- 1-MT treated (n=5) mice. *Cell counts were carried out using ImageJ software, and the average number of CD206+ IBA1- cells was counted in a randomly placed 4 x 10^4 μm^2 box, these data were presented +/- SEM. Data points in the plots represent data from one*

mouse. All the data were analysed using a post hoc Tukey HSD and Bonferroni's multiple comparison test using confidence limits of 95% (P= <0.05).*

No significant difference was found between the number of CD206+ IBA1- cells in non-tumour regions of the colon in the four treatment groups.

3.2.4. Loss of epithelial SOCS3 reduces the number of anti-tumorigenic M1 macrophages in tumour tissue

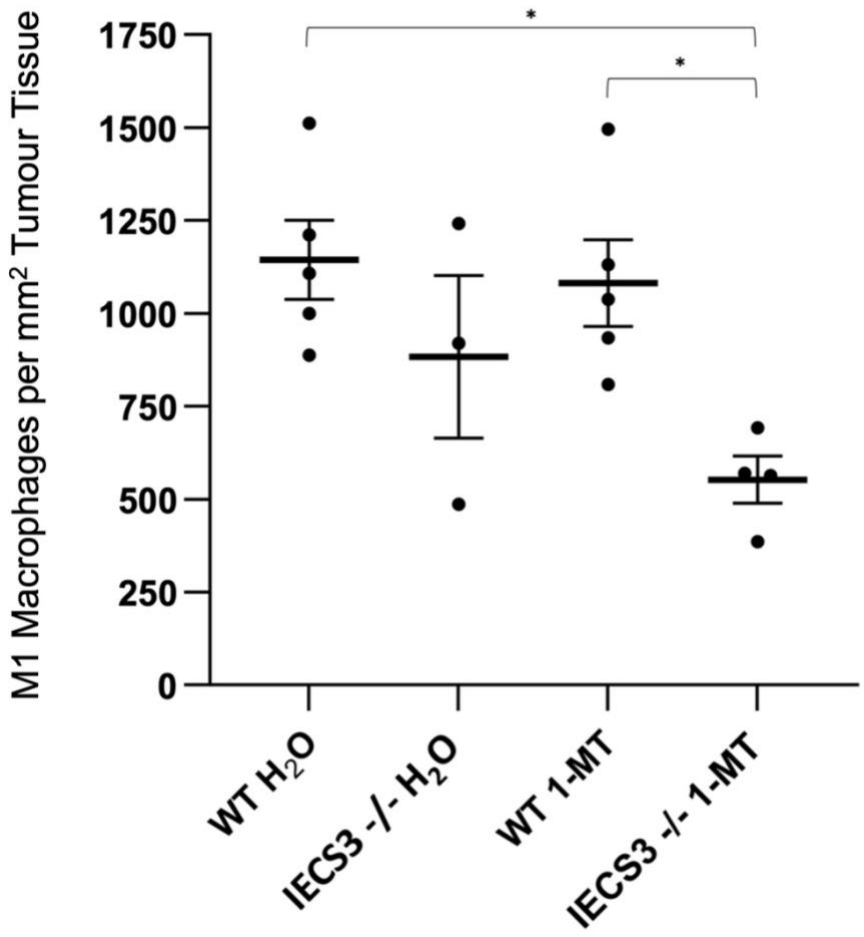

Figure 23. Average number of M1 macrophages per mm^2 tumour colon tissue in wildtype H_2O treated (n=5), wildtype 1-MT treated (n=4), IECS3 -/- H_2O treated (n=3), and IECS3 -/- 1-MT treated (n=4) mice. *Cell counts were carried out using ImageJ software, and the average number of M1 macrophages was counted per mm^2 tumour tissue, these data were presented +/- SEM. Data points in the plots represent data from one mouse. All the data*

were analysed using a post hoc Tukey HSD and Bonferroni's multiple comparison test using confidence limits of 95% (P=< 0.05).*

A significant difference between the number of M1 macrophages in wildtype vs IECS3 -/- tumour tissue treated with 1-MT was found.

3.2.5. Loss of IEC SOCS3 and/or 1-MT treatment does not affect the number of M2 macrophages found per mm^2 tumour tissue in the colon

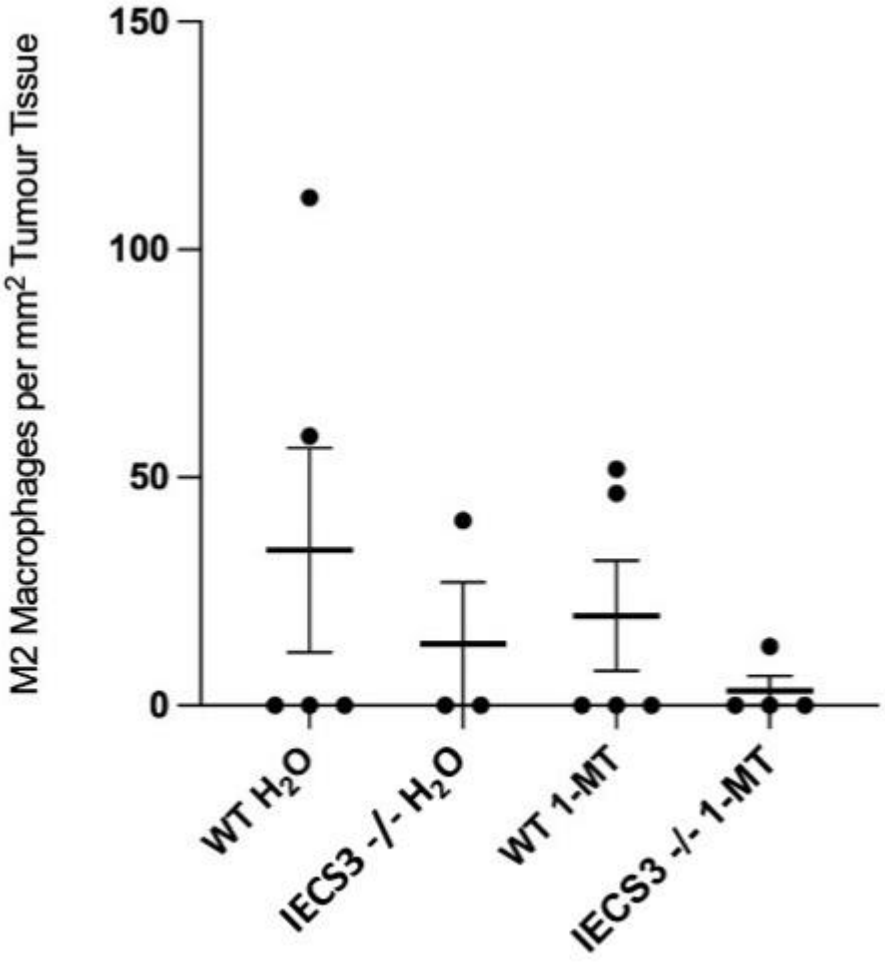

Figure 24. Average number of M2 macrophages per mm^2 tumour colon tissue in wildtype H_2O treated (n=5), wildtype 1-MT treated (n=4), IECS3 -/- H_2O treated (n=3), and IECS3 -/- 1-MT treated (n=4) mice. *Cell counts were carried out using ImageJ software, and the average number of M2 macrophages was counted per mm^2 tumour tissue, these data were presented +/- SEM. Data points in the plots represent data from one mouse. All the data*

were analysed using a post hoc Tukey HSD and Bonferroni's multiple comparison test using confidence limits of 95% (P= <0.05).*

No significant difference was found between the number of M2 macrophages in tumour regions of the colon in the four treatment groups.

3.2.6. Loss of epithelial SOCS3 increases the number of CD206+ IBA1- cells in tumour tissue and this is reversed through 1-MT treatment

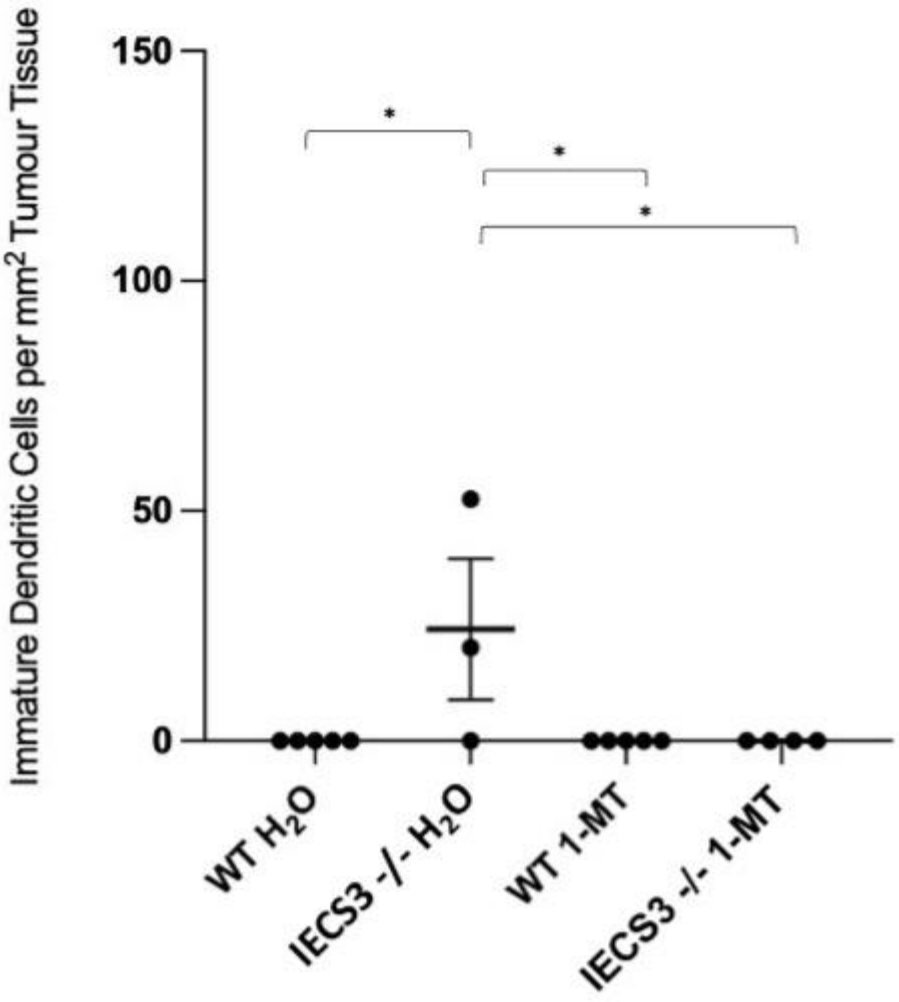

Figure 25. Average number of CD206+ IBA1- cells per mm^2 tumour colon tissue in wildtype H_2O treated (n=5), wildtype 1-MT treated (n=4), IECS3 -/- H_2O treated (n=3), and IECS3 -/- 1-MT treated (n=4) mice. *Cell counts were carried out using ImageJ software, and the average number of CD206+ IBA1- cells was counted per mm^2 tumour tissue, these data were presented +/- SEM. Data points in the plots represent data from one mouse. All the data*

were analysed using a post hoc Tukey HSD and Bonferroni's multiple comparison test using confidence limits of 95% (P=< 0.05).*

A significant difference was found between the number of CD206+ IBA1- cells in tumour regions of the colon in IECS3 -/- H_2O-treated mice compared to the other three groups.

3.3. Assessment of IDO activity

Our previous research assessing IDO protein expression via immunohistochemistry has shown IDO to be elevated in the IECS3 -/- tissue, however, this increase in protein expression does not necessarily indicate it is more active. Methods to assess IDO activity include measuring the ratio of metabolite vs. catabolite. IDO is an enzyme known to catalyse the breakdown of tryptophan into kynurenine. To measure the activity of this enzyme in mouse colon tissue, tryptophan and kynurenine expression was analysed using HPLC. Tryptophan expression was measured at an excitation wavelength of 297 nm and emission of 348 nm in agreement with previous literature (Lesniak et al., 2013). KYN, AA, 3-HK and 3-HAA expression was analysed at an excitation wavelength of 364 nm and emission of 480 nm and KYNA expression was measured at an excitation of 330 nm and emission of 390 nm. Calibration curves were produced using bio-inert software and compared to standards.

3.3.1. Tryptophan is detected in wildtype 1-MT treated colon tissue

a.

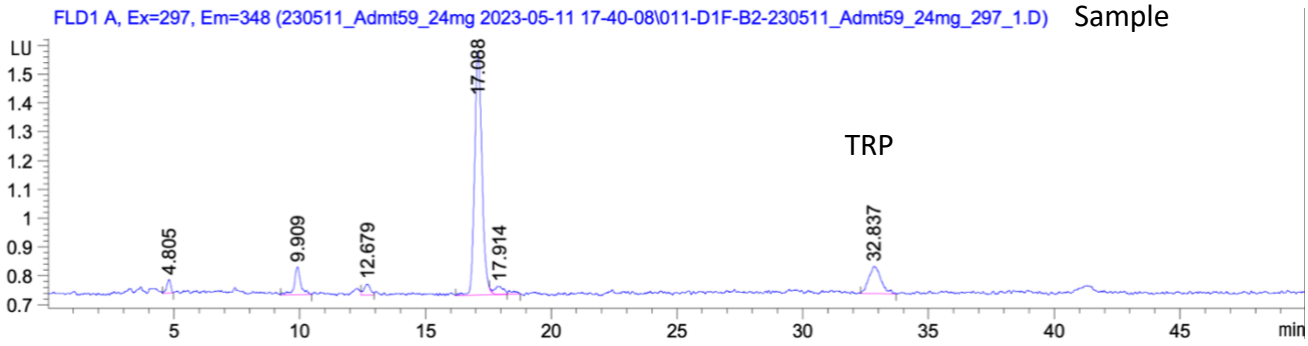

b.

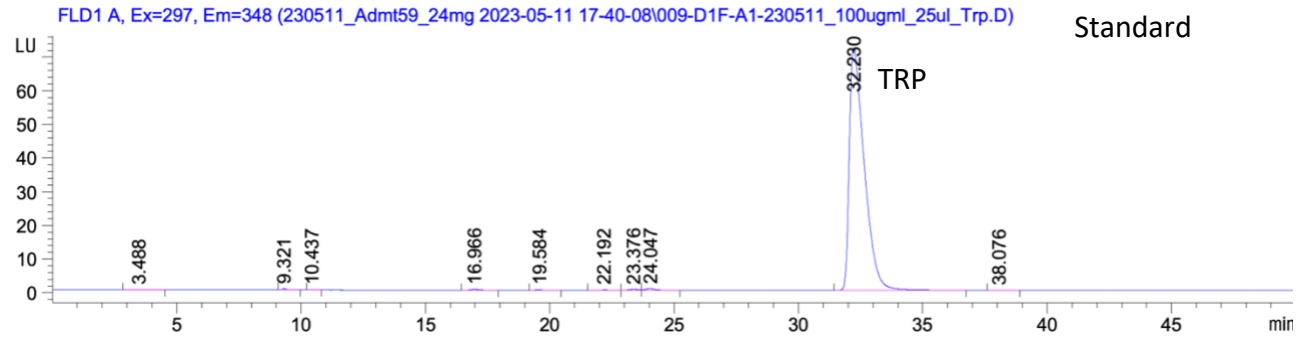

c.

	TRP
Retention Time of Standard	32.23
Retention Time of Sample	32.837
Area (LU*s)	3.15676
Metabolic Quantity (µg)	0.001987884
Mass of Sample (µg)	24000
Metabolite (µg)/ Sample (µg)	2.48486×10^{-6}

Figure 26. Tryptophan detection from 1-methyl tryptophan treated wildtype mouse colon tissue separated using HPLC at an excitation of 297 nm and emission of 348 nm. a. 24 mg colon sample, b. 100 µg/mL TRP standard sample and c. Calculations of the quantity of TRP in the sample. *The peak at 32.8 minutes in the sample indicates the presence of tryptophan as shown by comparison with the standard. No peaks were detected for* KYN, AA, 3-HK, 3-HAA and KYNA.

3.3.2. 3-Hydroxykynureneine is detected in wildtype 1-MT treated colon tissue

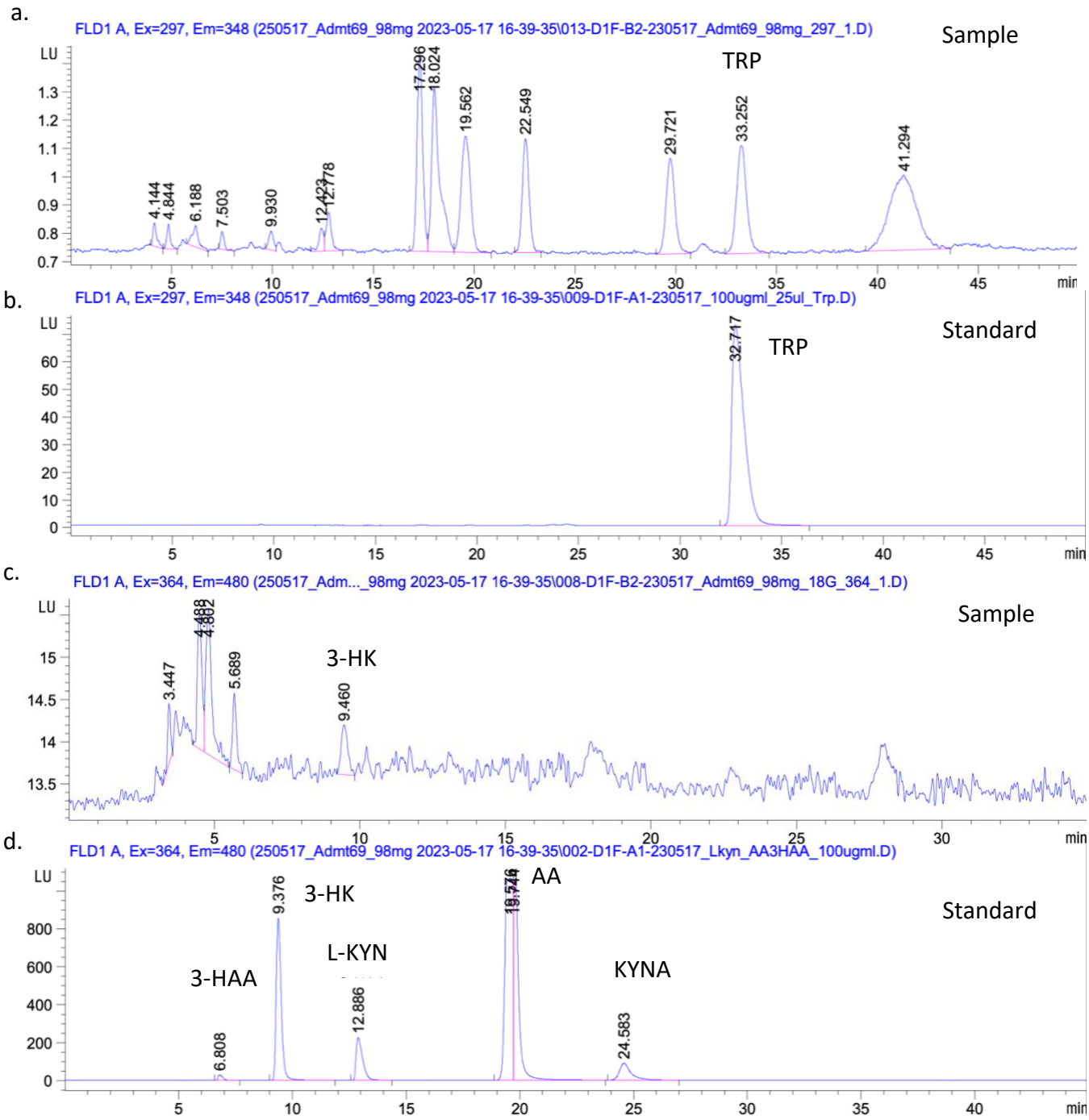

e.

	TRP	3-HK
Retention Time of Standard	32.717	9.376
Retention Time of Sample	33.252	9.46
Area (LU*s)	13.42925	9.40849
Metabolic Quantity (µg)	0.008456707	0.179825879
Mass of Sample (µg)	98000	98000
Metabolite (µg)/ Sample (µg)	2.58879×10^{-6}	5.50487×10^{-5}

Figure 27. Tryptophan and 3-hydroxykynurenine detection from 1-methyl tryptophan treated wildtype mouse colon tissue separated using HPLC. An excitation of 297 nm and emission of 348 nm was used for the detection of TRP, and an excitation of 364 nm and emission of 480 nm was used to detect 3-HK. a. 98 mg colon sample at 297 nm excitation, b. 100 µg/mL TRP standard sample at 297 nm excitation, c. 98 mg colon sample at 364 nm excitation, d. 100 µg/mL 3-HK standard sample at 364 nm excitation and e. Calculations of the quantity of TRP and 3-HK in the sample. *The peak at 33.3 minutes in the 297 nm excited sample indicates the presence of tryptophan as shown by comparison with the standard, and the peak at 9.5 minutes in the 364 nm excited sample indicates the presence of 3-HK as shown by comparison with the standard. No peaks were detected for* KYN, AA, 3-HAA and KYNA.

3.3.3. Tryptophan is detected in IECS3 -/- 1-MT treated colon tissue

a.

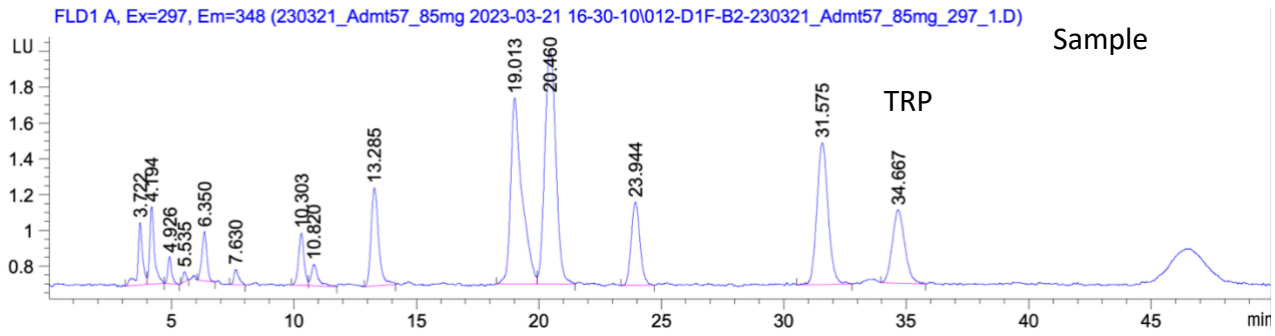

b.

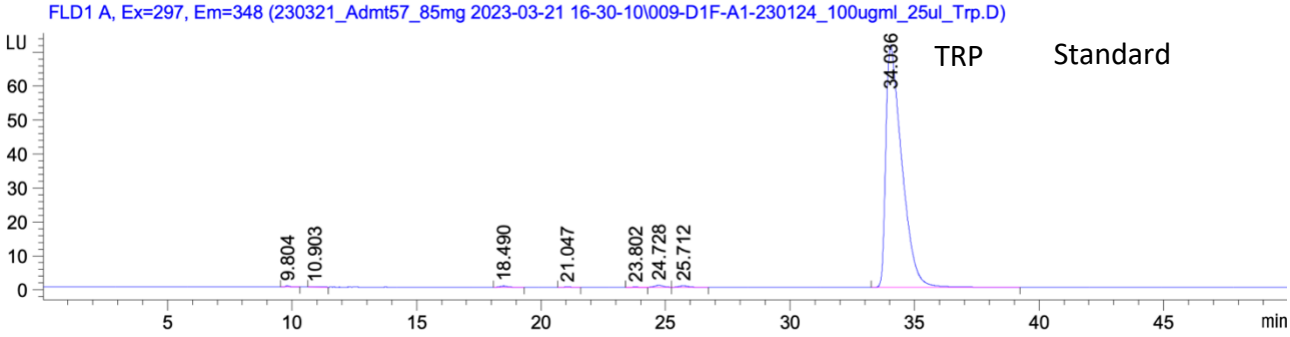

c.

	TRP
Retention Time of Standard	34.036
Retention Time of Sample	34.667
Area (LU*s)	14.48347
Metabolic Quantity (µg)	0.009120573
Mass of Sample (µg)	85000
Metabolite (µg)/ Sample (µg)	3.21903×10^{-6}

Figure 28. Tryptophan detection from 1-methyl tryptophan treated IECS3 -/- mouse colon tissue separated using HPLC at an excitation of 297 nm and emission of 348 nm. a. 85 mg colon sample, b. 100 µg/mL TRP standard sample and c. Calculations of the quantity of TRP in the sample. *The peak at 34.7 minutes in the sample indicates the presence of tryptophan as shown by comparison with the standard. No peaks were detected for* KYN, AA, 3-HK, 3-HAA and KYNA.

a.

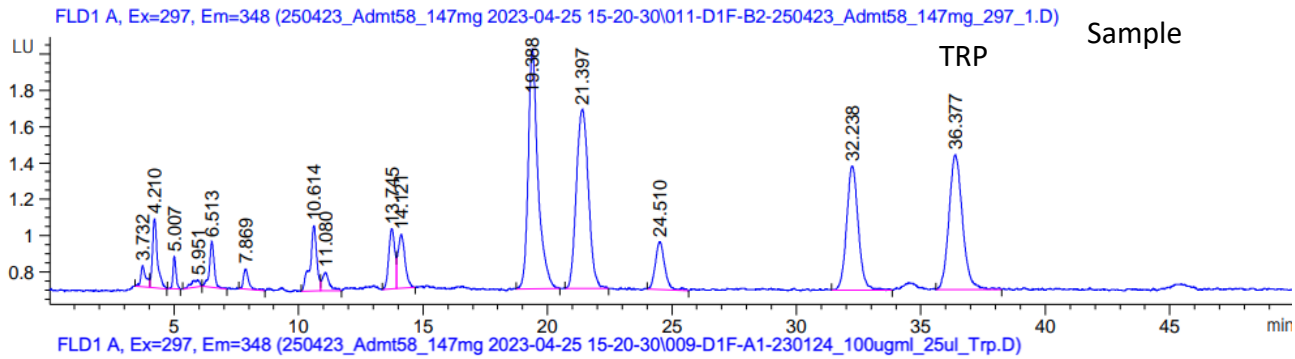

b.

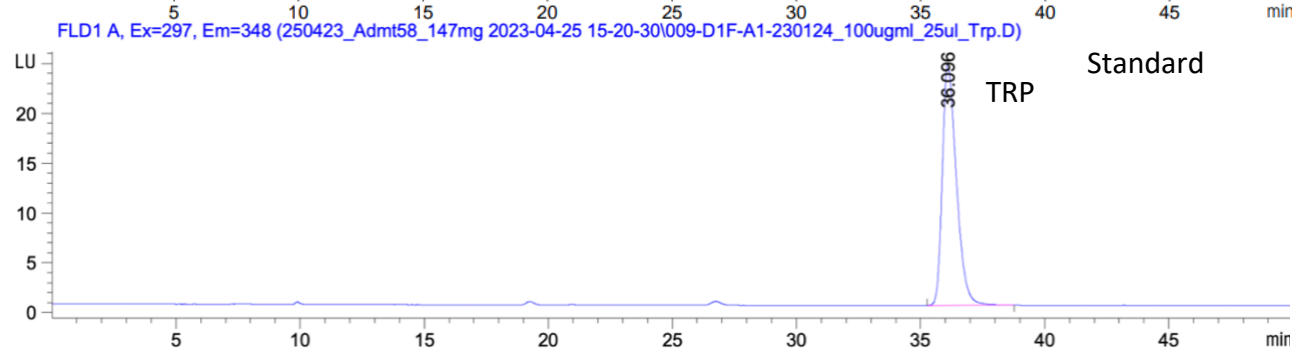

c.

	TRP
Retention Time of Standard	36.096
Retention Time of Sample	36.377
Area (LU*s)	28.13192
Metabolic Quantity (µg)	0.017715315
Mass of Sample (µg)	147000
Metabolite (µg)/ Sample (µg)	3.61537×10^{-6}

Figure 29. Tryptophan detection from 1-methyl tryptophan treated IECS3 -/- mouse colon tissue separated using HPLC at an excitation of 297 nm and emission of 348 nm. a. 147 mg colon sample, b. 100 µg/mL TRP standard sample and c. Calculations of the quantity of TRP in the sample. *The peak at 36.4 minutes in the sample indicates the presence of tryptophan as shown by comparison with the standard. No peaks were detected for* KYN, AA, 3-HK, 3-HAA and KYNA.

The HPLC findings show that tryptophan could only be detected at acceptable levels in the mouse-treated colon tissues. One sample detected 3-HK, and this is likely due to having an increased tissue mass >100mg. Unfortunately, this resulted in an inability to gather

kynurenine data from all four treatment groups, therefore any significant comparisons could not be made within the data.

3.4. Impact of 1-MT on polarisation of THP-1 Cells into M1/ M2 Macrophages

3.4.1. 1-MT treatment has no effect on the polarisation of THP-1 cells to M1 macrophages

THP-1 cells were polarised into M1 cells using a recognised method (Genin et al., 2015) with IFN-γ and LPS stimulation. 1-MT (1 and 0.25 μg/mL) was simultaneously administered to cells to see whether this affected polarisation as 1-MT is a known blocker of the enzyme IDO. Antibody marker iNOS was used to stain successfully polarised M1 macrophages.

A)

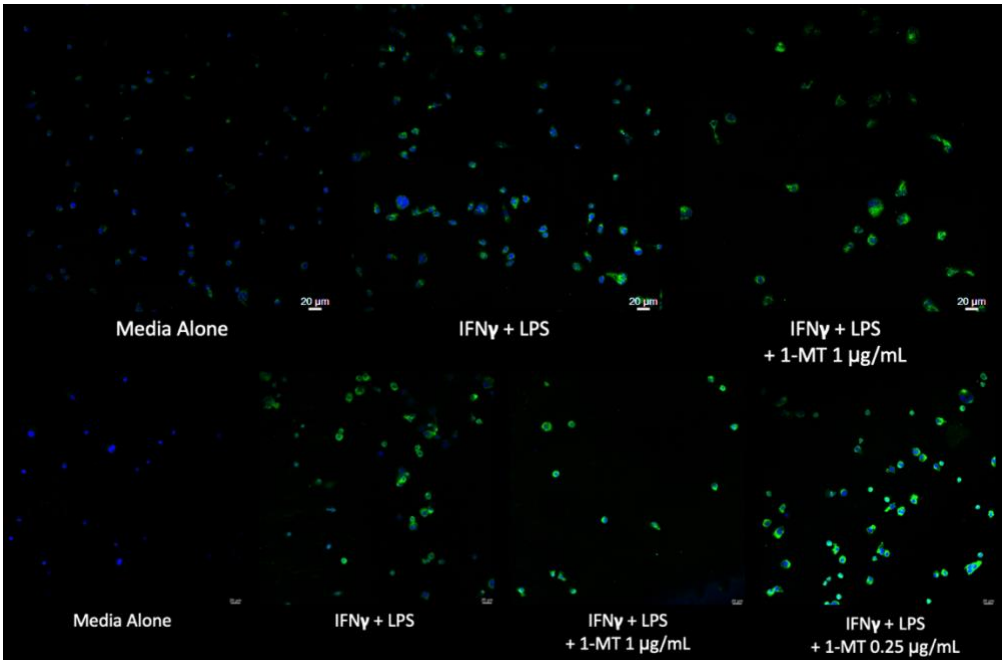

B)

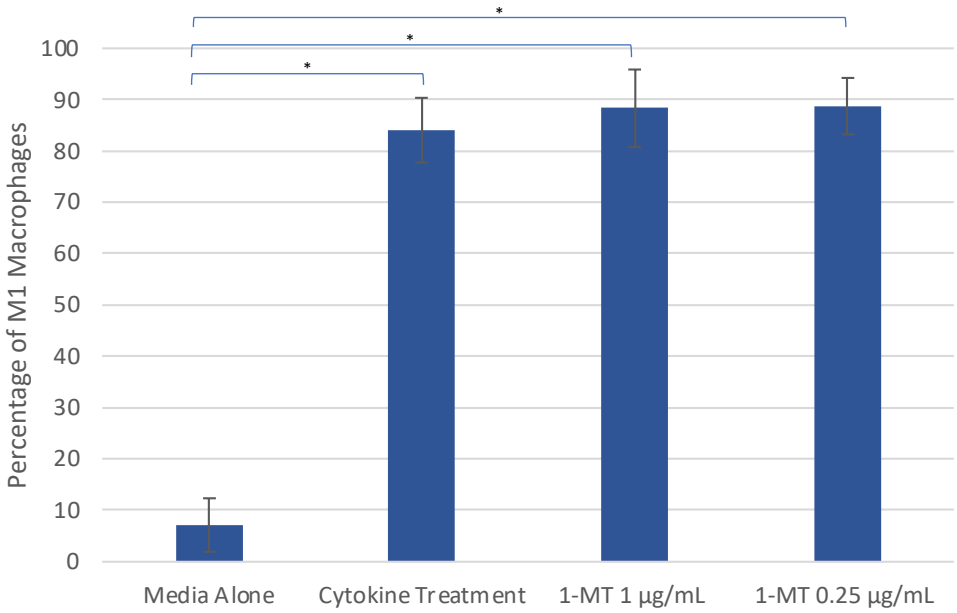

Figure 30. THP-1 cell polarisation into M1 macrophages with 20 ng/mL IFN-γ, 10 pg/mL LPS and 1/0.25 µg/mL 1-MT over a 24-hour period. *A) Following polarisation, cells were fixed and stained with iNOS antibody (Millipore, ABN26) before being incubated in secondary antibody AF488 (Invitrogen, 21206). Cells were mounted with DAPI and imaged using the Stellaris 5 confocal microscope at a magnification of 20x and aperture of 0.75. DAPI staining was imaged at an excitation wavelength of 405 nm (coloured blue) and iNOS staining was imaged at an excitation wavelength of 499 nm (coloured green). B) Cells were counted using ImageJ and presented +/- SD. Data were analysed using a one-way ANOVA and post hoc*

Tukey HSD and Bonferroni's multiple comparison test with confidence limits of 95% (P= <0.05) (n=3).*

Undifferentiated THP-1 cells expressed very little to no iNOS whereas differentiated cells expressed an average of 87% +/- SD of the M1-exclusive marker, indicating effective M1 macrophage polarisation. No significant difference was found between the polarised M1 macrophages treated with/without 1-MT; therefore 1-MT treatment had no effect on their polarisation.

3.4.2. 1-MT treatment has no effect on the differentiation of THP-1 cells to M2 macrophages

THP-1 cells were polarised into M2 cells with IL-4 and IL-13 stimulation (Genin et al., 2015). 1-MT (1 and 0.25 µg/mL) was simultaneously administered to cells to see how this affected polarisation. Antibody marker CD206 was used to stain successfully polarised M2 macrophages.

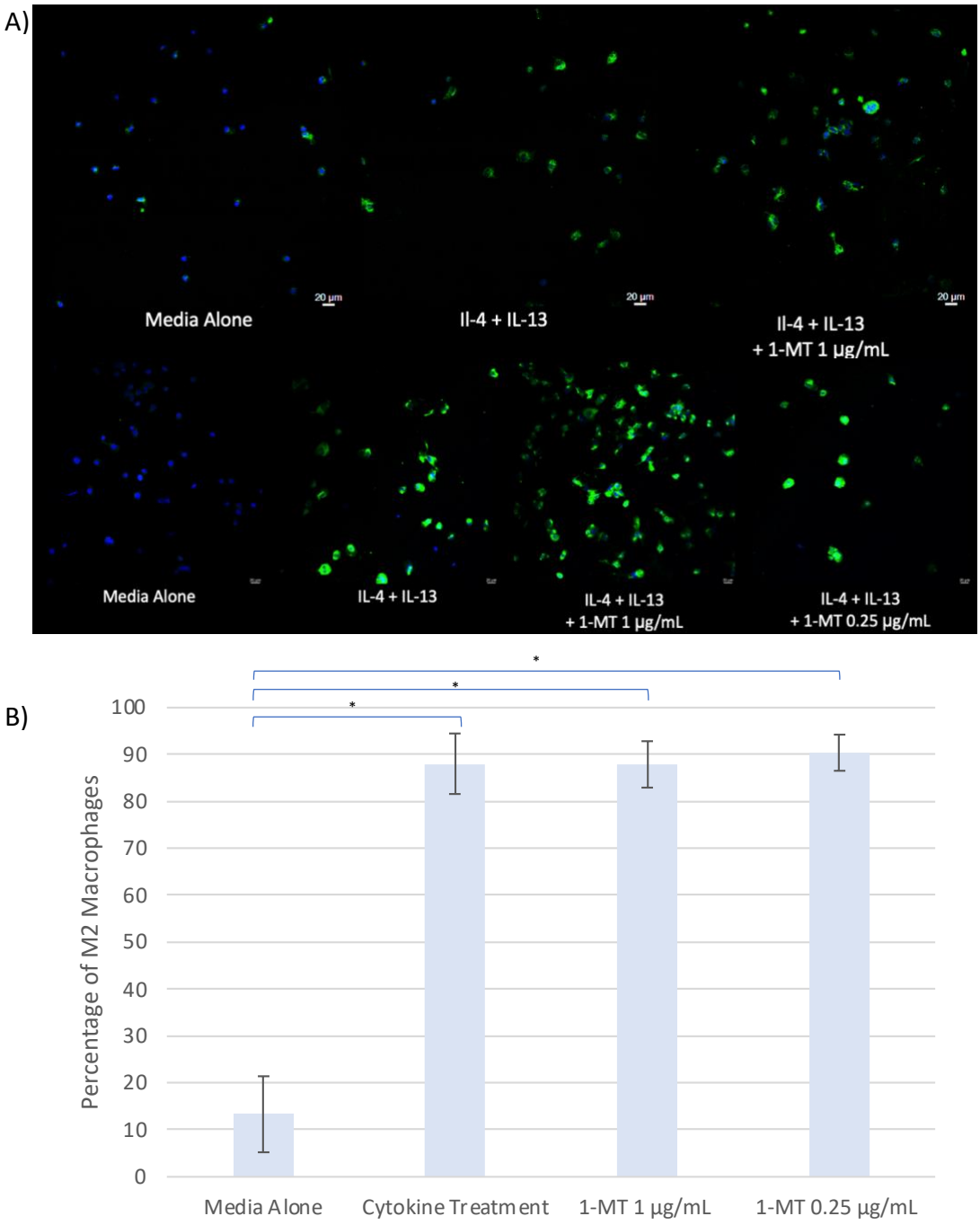

Figure 31. THP-1 cell polarisation into M2 macrophages with 20 ng/mL IL-4, 20 ng/mL IL-13 and 1/0.25 µg/mL 1-MT over a 48-hour period. *A) Following polarisation, cells were fixed and stained with CD206 antibody (Abcam, ab64693) before being incubated in secondary antibody AF488 (Invitrogen, 21206). Cells were mounted with DAPI and imaged using the Stellaris 5 confocal microscope at a magnification of 20x and aperture of 0.75. DAPI staining was imaged at an excitation wavelength of 405 nm (coloured blue) and CD206 staining was imaged at an excitation wavelength of 499 nm (coloured green). B) Cells were counted using ImageJ and presented +/- SD. Data were analysed using a one-way ANOVA and post hoc*

Tukey HSD and Bonferroni's multiple comparison test with confidence limits of 95% (P= <0.05) (n=3).*

Undifferentiated THP-1 cells expressed very little CD206 whereas differentiated cells expressed an average of 89% +/- SD of the M2-exclusive marker, indicating effective M2 macrophage polarisation. No significant difference was found between the polarised M2 macrophages treated with/without 1-MT; therefore 1-MT treatment had no effect on their polarisation.

3.5. Impact of 1-MT on macrophage expression of IDO and SOCS3

3.5.1. IDO expression may increase in M2 macrophages treated with 1-MT and decrease in M1 macrophages treated with 1-MT

Previous studies have suggested that M1 preferentially express SOCS3 and M2 express IDO (Wei et al., 2021). To determine what effect 1-MT was having on macrophage expression of IDO and SOCS3, polarised cells treated with/ without 1-MT were analysed on a western blot.

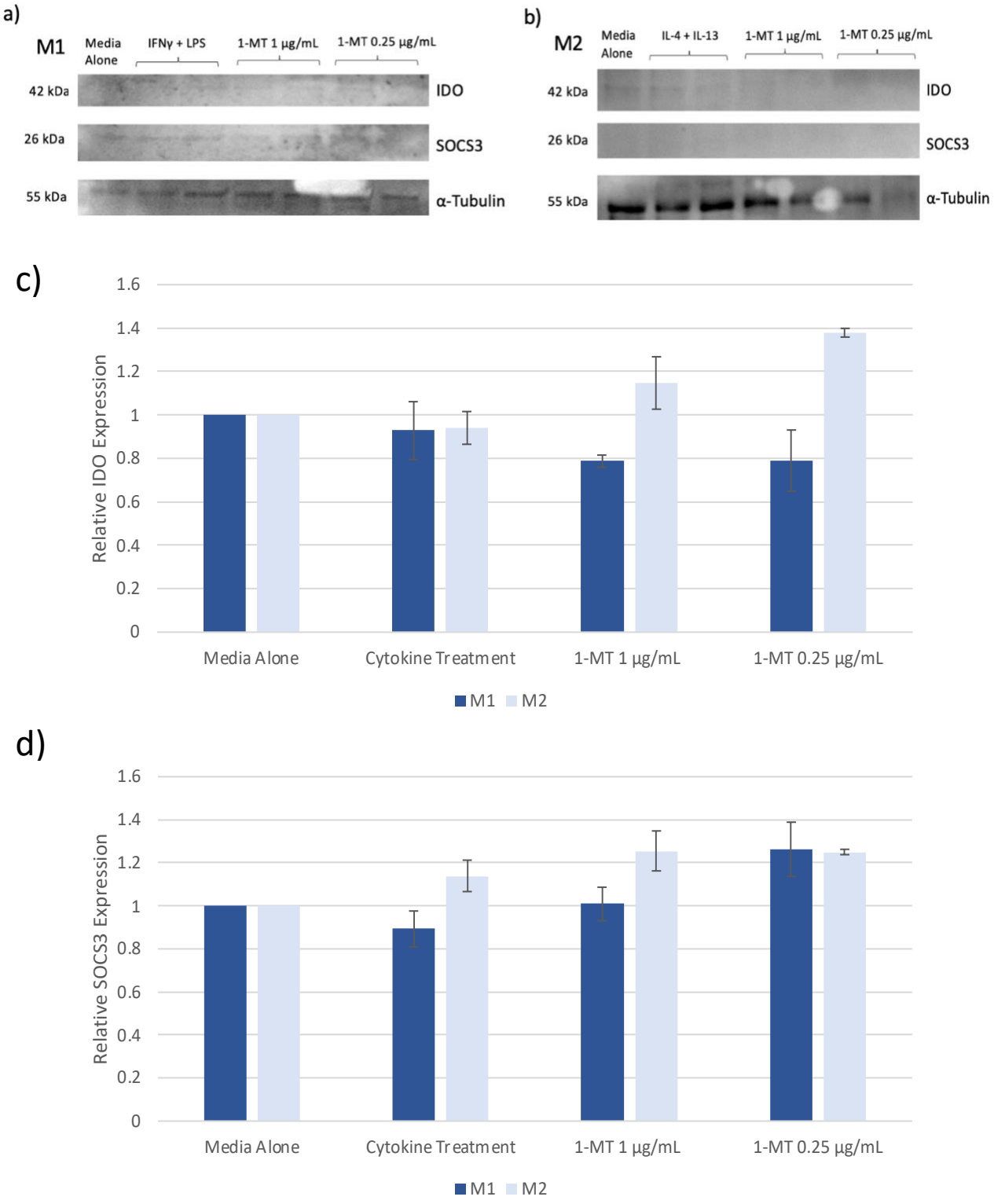

Figure 32. Cells were polarised into M1/ M2 macrophages using cytokine stimulation and given 1-MT treatment across a 24/ 48-hour period. *Cells were run on a gel and transferred to nitrocellulose membranes before being stained for SOCS3 (Cell Signalling Technology, 2932S) and IDO (Santa-Cruz Biotechnology, sc-137012). Blots were analysed using iBright*

Analysis Software and bands were normalised and the average for each treatment group (n=2) was calculated and made relative to unpolarised cells +/- SD. (n=1).

Statistical analysis was not possible due to a lack of biological replicates, but it appears there may be a decrease in the expression of IDO in 1-MT treated M1 macrophages compared to M1 cells without 1-MT treatment. The opposite can be seen for M2 macrophages, where IDO expression may increase in cells treated with 1-MT compared to without 1-MT treatment.

SOCS3 expression may have a tendency to increase in both M1 and M2 polarised macrophages treated with 1-MT compared to those that were not treated with 1-MT.

4. Discussion

4.1. Summary of Findings

The overall aims of this project were to investigate a potential explanation as to why IDO-inhibitor therapy did not result in consistent tumour growth inhibition in clinical trials, following very promising results in animal models. SOCS3 expression was identified as likely having importance in the management of IDO within humans, as this gene is often silenced in human tumours. We investigated how the loss of SOCS3 impacted the outcomes of IDO inhibitor therapy in a widely used animal model of CRC. Expression of IDO (as shown by Whittingham-Dowd et al. (in prep, 2024)) may be insufficient to determine its activity, we sought to measure metabolite (tryptophan) and catabolite (kynurenine) ratios in tumour and non-tumour colonic tissue, via HPLC, as a measure of enzyme activity. Finally, this thesis aimed to look at macrophage differentiation in culture and to determine the effects of IDO inhibitor on their polarisation into M1 (tumour-inhibiting) or M2 (tumour-promoting) phenotypes.

Tumours lacking SOCS3 (via conditional deletion in IEC) were found to be resistant to the anti-tumour effects of 1-MT treatment, possibly through the significantly reduced number of anti-tumorigenic M1 macrophages in tumour colon tissue compared to wildtype 1-MT treated (Whittingham-Dowd et al. (in prep, 2024)).

4.2. Impact of IECS3 -/- and IDO inhibition on macrophage phenotype in the colon

M1 and M2 macrophage counts were determined in non-tumour and tumour regions of mouse colon tissue through dual staining with IBA-1 (general macrophage marker) and CD206 (M2 macrophage marker) to determine whether loss of epithelial SOCS3 with/ without 1-MT treatment influenced intra-tumoral or lamina propria recruitment of macrophages.

In silico analysis showed that when the M1 macrophage marker, iNOS, is highly expressed CRC patients have better median survival results compared to low expression. This

corresponds to the pro-inflammatory response of M1 macrophages seen to induce immune cells to target tumours (Pernot et al., 2014). M1 macrophages expressing iNOS were found to upregulate SOCS3 expression when in a pro-inflammatory environment (Wilson, 2014). This relationship with M1 macrophages presents a novel role of SOCS3, as it acts to supress tumours. However, there are many mechanisms by which SOCS3 helps to mediate the immune response as it has been found to interact with a variety of different pathways (Carow & Rottenberg, 2014).

Additionally, analysis of the M2 macrophage marker, CD206, found that higher expression correlates with worse median survival (Lanczky & Gyorffy, 2021). These findings align with previous literature suggesting M2 macrophages are pro-tumorigenic, hence why M1 and M2 macrophages were quantified in this model (Boutilier & Elsawa, 2021).

Results indicated that loss of IEC SOCS3 with/without 1-MT does not affect the M1/M2 and CD206+ IBA1- cells (potential IDCs) in non-tumour regions. However, within the tumour microenvironment, a loss of epithelial SOCS3 significantly reduced the number of anti-tumorigenic M1 macrophages and increased the number of CD206+ IBA1- cells (potential IDCs). This supports literature that has noted the expression of SOCS3 up-regulates the maturation of DCs (Jiang et al., 2017). The reduction in M1 macrophages and increase in CD206+ IBA1- cells (potential IDCs) in the tumour microenvironment could be due to increased IDO. Studies have shown the increase in IDO results in regulatory T-cell formation as CD28 binding does not allow differentiation into effector cells due to the TRP starved state and leads to cell cycle arrest (Orabona et al., 2008). Macrophage recruitment has proven to be reduced in high IDO environments; however, this relationship was only studied in a fungal model therefore its application requires further analysis in additional models (Jiang et al., 2020). IDO is expressed by both DCs and macrophages (Bilir & Sarisozen, 2017; Struckmeier et al., 2023). It is notable that Struckmeier et al. (2023) identified the increased number of macrophages expressing IDO in the advanced tumour stages in oral squamous cell carcinoma, as this furthers the need to better understand the relationship between IDO and macrophages. The paper does not specify which macrophages, M1 (anti-tumour) or M2 (pro-tumour), have been found to express the IDO, this could be supportive or contradictory to the suggestion that increased IDO is the cause of reduced M1 macrophages. Choe et al.

(2014) identified this IDO expression, in Hodgkin lymphoma, from M2 macrophages. With the current understanding of macrophage polarisation, this conclusion supports the implied relationship between IDO and M1 macrophages. With this under consideration, the findings of this paper support the Whittingham-Dowd et al. (in preparation, 2024) theory that silencing of SOCS3 could reduce the efficacy of IDO inhibitor therapy, due to the over-expression of IDO, acting as a 'sink' for the inhibitor therapy. This is supported by the observation that M1 macrophages represent the immune response effectively counteracting the tumour, which is not achieved under IDO inhibiting treatment when SOCS3 has been silenced. Increasing the inhibitor dosage may mitigate SOCS3 silencing, but IDO/tryptophan metabolism is important in many biological systems, from brain chemistry to immunity to pathogens (Moffett & Namboodiri, 2003; Richard et al., 2009). Increasing the dose to overcome the increased tryptophan metabolism may cause many side-effects of unknown outcome.

Struckmeier et al. (2023) also referred to the idea that the Mills Paradigm definition of M1 and M2 macrophages may not be consistent across all tumours and presented the need to review the model's application (Mills et al., 2000). In addition to this Jayasingam et al. (2020) are in agreement, that the binary classification of macrophages is not a good representation of the spectrum that could be used to define macrophage polarisation. Further investigation into macrophage polarisation could weaken the view of M1 and M2 macrophages being specifically anti/pro-tumorigenic, respectively, because there are many subsets between these distinctions which display characteristics of both M1/M2 macrophages.

Furthermore, immature DCs have been known to have pro-tumorigenic effects as they are unable to activate T-cells, effectively causing an environment in which the cancerous cells have greater tolerance to the immune response (Dudek et al., 2013). IDO and SOCS3 play antagonistic roles in the maturation of DCs as IDO acts in preventing T-cell proliferation by restricting the ability of DCs to mature, creating a more tolerant environment for tumours (Bracho-Sanchez et al., 2020). Whereas, SOCS3 expression has proven to up-regulate DC activation (Jiang et al., 2017). This is supported by the findings in this study as the CD206+ IBA1- cells (potential IDCs) were greater in numbers in the IECS3 -/- tumour tissue of water

controls. Jiang et al. (2017) also found that the impact of SOCS3 on DCs may be altered depending on the enzymes present, theorising its ability to aid and prevent their maturation. This presents a potential route for further analysis, as the impact of different immune environments is likely to change whether SOCS3 is viable for use as a biomarker before administering IDO inhibition immunotherapy techniques. Interestingly, in this study, administering 1-MT found that the increase of CD206+ IBA1- cells (potential IDCs) in the IECS3 -/- water treated tumour tissue was no longer apparent. Agaugué et al. (2006) identified that the relationship between 1-MT and DCs was not likely to be direct, as engaging different stimuli in the presence of 1-MT produced varied maturation results. The study also concluded that 1-MT could be interacting with targets other than IDO, which in turn could impact the function of DCs. In the context of this study, it is unclear why the addition of 1-MT resulted in a reduction in CD206+ IBA1- cells (potential IDCs), but it could be explained by the findings in Agaugué et al. (2006).

4.3. Assessment of IDO activity

Previous research suggested IDO protein increases in SOCS3 deficient tumours. However, an increase in enzyme protein expression does not indicate it is active (Whittingham-Dowd et al., in preparation 2024). This study aimed to optimise a method by which IDO activity could be measured in colon tissue by measuring the ratio of metabolite vs. catabolite of IDO. IDO catalyses the breakdown of TRP to KYN, therefore a higher amount of KYN vs. TRP would suggest there is greater IDO activity in the tissue and more immune tolerance due to the 'TRP starved state' produced in cells leading to reduced patient survival (Bilir & Sarisozen, 2017; Orabona et al., 2008). Therefore, the expression of both TRP and KYN was analysed using HPLC with IECS3 -/- tissue treated with/ without 1-MT.

This study validated the presence of TRP in wildtype 1-MT treated and IECS3 -/- 1-MT treated mouse colon tissue as a peak was observed where expected at an excitation wavelength of 297 nm and emission of 348 nm and this aligned with previous research (Lesniak et al., 2013). A peak was also identified as 3-HK in wildtype 1-MT treated tissue where expected. These peaks suggest that the method does identify the presence of both the metabolite and catabolite of IDO and could prove successful in identifying IDO activity.

However, this study was limited due to a lack of samples for each study group, along with a small sample weight for the available tissue, therefore no significant data was produced. In addition to this, the preparation of tissue before HPLC was a lengthy process with multiple routes of contamination meaning often the tissue would become non-functional as inaccurate data would be produced. Development of the method may provide routes to minimise opportunities for contamination to occur and reduce the amount of waste tissue created during testing.

4.4. Macrophage polarisation in vitro

Macrophage polarisation is an important, well-regulated process which allows the body to fight disease, an imbalance in this polarisation has been associated with many inflammatory conditions (Wang et al., 2014). THP-1 cells, derived from a human leukaemia monocytic cell line are useful for studying macrophages and their polarisation. THP-1 cells were polarised into M1 pro-inflammatory macrophages using IFN-γ and LPS, and M2 pro-tumorigenic macrophages using IL-4 and IL-13 following a method by Genin et al. (2015). These cells were simultaneously treated with/ without 1-MT to see whether this influenced their ability to polarise into either M1/M2 cells. Their polarisation was then measured using markers iNOS (M1 macrophage marker) and CD206 (M2 macrophage marker) via confocal microscopy. The data showed that this method of polarisation was effective in producing M1/M2 macrophages expressing their appropriate marker compared to unstimulated cells. However, when treated with 1-MT, no differences were seen in their polarisation, suggesting that 1-MT treatment does not affect macrophage polarisation.

Jiang et al. (2020) found that when mice were infected with *Aspergillus fumigatus*, there was a decrease in the expression of M1 factors such as IFN-γ and an increase in M2 inflammatory factors such as IL-10 when pre-treated with 1-MT compared to mice without 1-MT pre-treatment. This contradicts the suggestion that 1-MT does not have an impact on macrophage polarisation, to the extent that 1-MT can in fact promote M2 polarisation. Yu et al. (2023) further investigated this relationship, with a focus on regulating the CCL2 and CCR2 signalling pathway within the fungus, finding that 1-MT increased expression of the chemokine ligand and its receptor within *A. fumigatus* and found an increase in CD206+

macrophages. CCL2-CCR2 mechanisms are also present in various cancers, including colorectal (Xu et al., 2021). A greater understanding of how 1-MT interacts with this signalling pathway within cancer could identify treatment markers, in addition to SOCS3, to prioritise patients for particular immunotherapies.

Previous research has shown that IDO increases the expression of M2 markers such as IL-10 and knocking out IDO results in an increase in the expression of M1 markers and a decrease in M2 markers (Wang et al., 2014). This highlights the significance of IDO expression on macrophage polarisation and its importance in immune regulation. Hence, this study investigated the expression of IDO and SOCS3 by macrophages with/ without 1-MT. To do this, polarised cells were analysed via western blot. IDO expression appears to increase in M2 macrophages treated with 1-MT and decrease in M1 macrophages treated with 1-MT compared to those without 1-MT. SOCS3 expression may have a tendency to increase in both M1 and M2 polarised macrophages treated with 1-MT compared to those without 1-MT. However, no significant conclusions could be drawn from the data due to a lack of biological replicates.

In a fungal model studied by Wei et al. (2021), it was found that overexpression of SOCS3 in THP-1 macrophages promotes M1-like polarisation. There has also been confirmation that M2 macrophages express IDO (Choe et al., 2014). This presents a base of understanding of the relationships between macrophages, IDO and SOCS3 but comes with limitations due to how the results can be applied to human CRCs. The two papers display how interactions differ within a fungal infection of *Talaromyces marneffei* in THP-1 macrophages and Hodgkin lymphoma in stromal cells, this only provides a suggestion as to how the macrophage expression may occur within CRC. This is a key distinction to make as it is known that among tumours there is a complex difference between microenvironments (Tirosh et al., 2016).

Additionally, many papers have noted that negative polarisation of M1-like macrophages is associated with SOCS3 expression within mouse bone marrow (Qin et al., 2012; Wei et al., 2021; Yan et al., 2013). This contradicts the suggestion that M1 macrophages exclusively prioritise SOCS3 expression. Ultimately, a clear view of definite macrophage polarisation is likely not possible without reassessing how they a classified as present by numerous

macrophage studies (Jayasingam et al., 2020; Struckmeier et al., 2023). With a wider spectrum of macrophage polarisation may come greater clarity over how SOCS3 and IDO expression differs within cancers and how this can be used, alongside the development of standardised biomarkers to better prescribe treatment.

Further research is needed to investigate SOCS3 expression because it appears inconsistent across different cancer types. A study by Dai et al. (2022) provides evidence that suggests SOCS3 mRNA overexpression has been known to be promoted within lymphoma, glioma, and oesophageal cancer, whereas under-expression was associated with lung, bladder cancer and leukaemia.

4.5. Limitations and Future Directions

The discussed findings present a potentially increased understanding of the relationship between SOCS3 and IDO and the mechanisms by which they interact. However, there are limitations that require further investigation before conclusive statements can be made. Awareness of the limiting factors generates the next steps to achieving a clear view of how the mechanisms may improve current immunotherapy techniques and make them more accessible.

Initial limitations are found within the AOM/DSS model itself, where tumours have been forced rather than being allowed to develop naturally. Developing tumours this way in the mice raises the question as to whether it is a good model for a naturally occurring cancer, and whether it would display the same tumour immune environment and interact with the immune system in the same way. Studies suggest the AOM/DSS mice model is a ‘powerful’ method to use when studying the pathogenesis of CRC (Parang et al., 2016). However, there is not enough data to suggest that this mechanism of CRC induction does not have an effect on the immune environment in the same way it would in naturally occurring tumours.

The mice in this model were treated with 1 mg/mL 1-MT as a set value, to deepen understanding of how this drug works, alternate concentrations could be used to get a drug-dose response and see trends within the data in this model and the impact this has on the

immune environment. In the future, 1-MT could also be trialled with other more traditional drugs like chemotherapy to see if this influences the immune environment and allows a strong treatment plan to be developed for those it would likely benefit. Progression through drug trials would also offer the opportunity to identify likely side-effects of various administered doses.

Staining of macrophages of the colon tissue is good for allowing visualisation of where they are localised, but it is not the best method to quantify cells in a tissue. Some of the variations seen in macrophage numbers may be due to a lack of consistency in the exact location within the tumour visualised in the narrow section of tissue. Flow cytometry would give a better enumeration but would rely on precise excision of the tumour to reduce variability. More research into their activation and movement into the tumours in the IECS3 -/- mice is required before any distinct conclusions can be drawn. The M1/M2 markers chosen for this study were IBA-1, a general macrophage marker, and CD206 an M2 macrophage marker. IBA-1, a cytoplasmic protein, stains microglial/ macrophage cells and can display active and resting cells, this makes it a good macrophage marker (Ito et al., 1998). CD206, a cell surface protein, is normally expressed on M2 macrophages and immature DCs (Xu et al., 2020). However, as previously mentioned, the characterisation of macrophages is complex as there are many different subsets as opposed to being specifically M1 or M2 and some of these subsets can display characteristics of both types of macrophages, therefore this makes staining for one type more difficult (Jayasingam et al., 2020; Struckmeier et al., 2023). More macrophage markers could be trialled in future to confirm the findings of this study.

When investigating IDO activity, the method could be further optimised to prevent contamination of samples during preparation, reducing the likelihood of non-functional samples. By increasing the sample weight and the number of different samples, IDO activity measurement is possible because this study shows that IDO metabolites do produce peaks using this method.

Western blotting techniques utilise cell lysate to provide an average expression where all cells are quantified. Flow cytometry could have also been used to generate quantitative

results for single cells, future studies could seek to assess the western blot outputs for their accuracy. In future, the method would be repeated to gain biological replicates to help establish SOCS3/ IDO expression and macrophage polarisation.

The overall findings of this study suggest there is potential for immunotherapy biomarkers, such as SOCS3, which could help to improve stratification of patients for therapies that are likely to be more effective. Applying similar approaches to other carcinomas may lead to a more developed picture of the pathways by which SOCS3 and IDO interact, presenting new targets to improved cancer treatments. Increased knowledge of the tumour microenvironment may assist in building further awareness as to how external factors impact cancer development and treatment. Additionally, identifying the markers for successful treatment would save time for patients who would not benefit from IDO inhibition therapy, allowing them to try other methods that better improve their chances of survival.

Appendix 1

Cell Lysis Buffer, 500 mL

-4.4 g 150 mM sodium chloride

-3.9 g 50 mM Tris-HCl, pH 7.4

-0.15 g 1 mM ethylenediaminetetraacetic acid (EDTA)

-5 mL Triton X-100 (Sigma, T8787)

-0.6 g 3mM sodium deoxycholic acid

-0.5 g sodium dodecyl sulphate

-Add dH_2O to get a final volume of 500 mL

-Add protease inhibitor (Sigma, P8340) 5 µL for every 1 mL lysis buffer and phosphatase inhibitor cocktail IV (Fisher Chemical, 1285-1650) 10 µL for every 1 mL just before use

Genotyping Buffer, 200 mL

-0.4 mL 0.5 M EDTA (Invitrogen, 15576-028)

-10 mL 1 M pH 8.0 Tris-HCl

-0.8 mL 5 M NaCl

-2 mL Tween-20 (Sigma, p1379)

-186.8 mL sterile H_2O

Laemmli SDS-PAGE Running Buffer 1x, 1 litre

-100 mL 10x tris-glycine-SDS (TGS) running buffer (Bio-Rad, 161-0732)

-900 mL dH_2O

PBS + 0.25% Triton X-100, 50 mL

-50 mL 1x PBS

-125 µL Triton X-100

Tris-Borate-EDTA (TBE) Buffer, 1 litre

-108 g Tris base (Formula weight: 121.14 g) (Sigma-Aldrich, T4661)

-55 g Boric Acid

-40 mL 0.5 M EDTA

-Add dH_2O to get a final volume of 1 litre

TBS 10x (concentrated Tris-Buffered Saline), 1 litre

-24.2 g Tris base (Formula weight: 121.14 g)

-87.6 g NaCl (Formula weight: 58.4 g)

-Dissolve in 900 mL dH_2O.

-pH to 7.6 with Conc. HCl and add dH_2O to a final volume of 1 litre.

For a 1x solution, mix 1 part of the 10x solution with 9 parts dH_2O and pH to 7.6 again.

The final molar concentrations of the 1x solution are 20 mM Tris and 150 mM NaCl.

TBS + 0.25% Triton X-100, 50 mL

-50 mL 1x TBS

-125 µL Triton X-100

TBS + 0.025% Triton X-100, 50 mL

-50 mL 1x TBS

-12.5 µL Triton X-100

TBS + 0.01% Tween-20, 1 litre

-100 mL 10x TBS

-900 mL dH_2O

-100 µL Tween-20

Transfer Buffer, 1 litre

-200 mL Trans-Blot Turbo 5% Transfer Buffer (Bio-Rad, 10026938)

-200 mL 100% EtOH

-600 mL dH_2O

Tris-EDTA pH 9.0 buffer, 1 litre

-1.21 g Tris base

-0.37 g EDTA

-Dissolve in 1000 mL dH_2O

-pH to 9.0 with Conc. HCl

-Add 0.5 mL Tween-20 and mix well

-Store at room temperature for 3 months or at 4˚C for long term storage.

1% BSA in TBS, 100 mL

-BSA: 1.0 g (Sigma, A3059)

-1x TBS: 100 mL

-Store at 2-5˚C for up to 1 month or make 1.5 mL aliquots and store at -20˚C for up to 6 months.

2% BSA in PBS, 100 mL

-BSA: 2.0 g (Sigma, A3059)

-1x PBS: 100 mL

-Store at 2-5˚C for up to 1 month or make 1.5 mL aliquots and store at -20˚C for up to 6 months.

3% BSA in TBS, 100 mL

-BSA: 3.0 g

-1x TBS: 100 mL

-Store at 2-5˚C for up to 1 month or make 1.5 mL aliquots and store at -20˚C for up to 6 months.

5% BSA in TBS, 100 mL

-BSA: 5.0 g

-1x TBS: 100 mL

-Store at 2-5˚C for up to 1 month or make 1.5 mL aliquots and store at -20˚C for up to 6 months.

4% Paraformaldehyde in PBS, 100 mL

-Paraformaldehyde: 4.0 g

-1x PBS: 100 mL

-Store at 2-5˚C and avoid contact with light.

References

Agaugué, S., Perrin-Cocon, L., Coutant, F., André, P., & Lotteau, V. (2006). 1-Methyl Tryptophan Can Interfere with TLR Signalling in Dendritic Cells Independently of IDO Activity. *Journal of Immunology*, 177(4), 2061–2071.

Alzahrani, S. M., Al Doghaither, H. A., & Al-Ghafari, A. B. (2021). General Insight into Cancer: An Overview of Colorectal Cancer. *Molecular and Clinical Oncology*, 15(6), 271.

Bilir, C. & Sarisozen, C. (2017). Indoleamine 2,3-dioxygenase (IDO): Only an enzyme or a checkpoint controller? *Journal of Oncological Sciences*, 3(2), 52-56.

Boutilier, A. J., & Elsawa, S. F. (2021). Macrophage Polarization States in the Tumour Microenvironment. *International Journal of Molecular Sciences*, 22(13).

Bracho-Sanchez, E., Hassanzadeh, A., Brusko, M. A., Wallet, M. A., & Keselowsky, B. G. (2019). Dendritic Cells Treated with Exogenous Indoleamine 2,3-Dioxygenase Maintain an Immature Phenotype and Suppress Antigen-specific T-cell Proliferation. *Journal of Immunology and Regenerative Medicine*, 5.

Cabrera, C. M., Jiménez, P., Cabrera, T., Esparza, C., Ruiz-Cabello, F., & Garrido, F. (2003). Total loss of MHC class I in colorectal tumours can be explained by two molecular pathways: beta2-microglobulin inactivation in MSI-positive tumours and LMP7/TAP2 downregulation in MSI-negative tumours. *Tissue Antigens*, 61(3), 211 219.

Cancer Research UK. (2022). Bowel Cancer Screening. [Online]. Cancer Research UK. Last Updated: 06 April 2022. Available at: https://www.cancerresearchuk.org/about cancer/bowel-cancer/getting-diagnosed/screening [Accessed 19 November 2023].

Carow, B. & Rottenberg, M. E. (2014). SOCS3, a major regulator of infection and inflammation. *Frontiers in Immunology,* 5, 77374.

Choe, J. Y., Yun, J. Y., Jeon, Y. K., Kim, S. H., Park, G., Huh, J. R., Oh, S., & Kim, J. E. (2014). Indoleamine 2,3-dioxygenase (IDO) is frequently expressed in stromal cells of Hodgkin lymphoma and is associated with adverse clinical features: a retrospective cohort study. *BMC cancer*, 14, 335.

Coca, S., Perez-Piqueras, J., Martinez, D., Colmenarejo, A., Saez, M. A., Vallejo, C., Martos, J. A., & Moreno, M. (1997). The prognostic significance of intratumoral

natural killer cells in patients with colorectal carcinoma. *Cancer*, 79(12), 2320–2328.

Croker, B. A., Krebs, D. L., Zhang, J. G., Wormald, S., Willson, T. A., Stanley, E. G., Robb, L., Greenhalgh, J. C., Irmgard, F., Clausen, E. B., Nicola, A. N., Metcalf, D., Hilton, J. D., Roberts, W. A., & Alexander, S. W. (2003). SOCS3 negatively regulates IL-6 signalling in vivo. *Nature Immunology,* 4(6), 540–545.

Dai, L., Li, Z., Tao, Y., Liang, W., Hu, W., Zhou, S., Fu, X., & Wang, X. (2021). Emerging roles of suppressor of cytokine signalling 3 in human cancers. *Biomedicine & pharmacotherapy,* 144, 112262.

Dai, L., Tao, Y., Shi, Z., Liang, W., Hu, W., Xing, Z., Zhou, S., Guo, X., Fu, X., & Wang, X. (2022). SOCS3 Acts as an Onco-immunological Biomarker with Value in Assessing the Tumour Microenvironment, Pathological Staging, Histological Subtypes, Therapeutic Effect, and Prognoses of Several Types of Cancer. *Frontiers in Oncology*, 12.

Dudek, A. M., Martin, S., Garg, A. D., & Agostinis, P. (2013). Immature, Semi-Mature, and Fully Mature Dendritic Cells: Toward a DC-Cancer Cells Interface That Augments Anticancer Immunity. *Frontiers in Immunology*, 4.

Edin, S., Wikberg, M. L., Dahlin, A. M., Rutegård, J., Öberg, Å., Oldenborg, A., & Palmqvist, R. (2012). The Distribution of Macrophages with a M1 or M2 Phenotype in Relation to Prognosis and the Molecular Characteristics of Colorectal Cancer. *PLOS ONE*, 7(10), e47045.

Edin, S., Wikberg, M. L., Rutegård, J., Oldenborg, P. A., & Palmqvist, R. (2013). Phenotypic skewing of macrophages in vitro by secreted factors from colorectal cancer cells. *Public Library of Science One*, 8(9), 74982.

Emanuelli, B., Peraldi, P., Filloux, C., Sawka-Verhelle, D., Hilton, D., & Van Obberghen, E. (2000). SOCS-3 is an insulin-induced negative regulator of insulin signalling. *The Journal of Biological Chemistry*, *275*(21), 15985–15991.

Fearon, E. R., & Vogelstein, B. (1990). A genetic model for Colorectal tumorigenesis. *Cell,* 61(5), 759-767.

Fujiwara, Y., Kato, S., Nesline, M. K., Conroy, J. M., DePietro, P., Pabla, S., & Kurzrock, R. (2022). Indoleamine 2,3-dioxygenase (IDO) inhibitors and cancer immunotherapy. *Cancer Treatment Reviews*, 110, 102461.

Genin, M., Clement, F., Fattaccioli, A., Raes, M., and Michiels, C. (2015). M1 and M2

macrophages derived from THP-1 cells differentially modulate the response of cancer cells to etoposide. *BMC Cancer*, 15(577), 1-14.

Golshani, G., & Zhang, Y. (2020). Advances in immunotherapy for colorectal cancer: a review. *Therapeutic Advances in Gastroenterology*, 13, 1756284820917527.

Günther, J., Däbritz, J., & Wirthgen, E. (2019). Limitations and Off-Target Effects of Tryptophan-Related IDO Inhibitors in Cancer Treatment. *Frontiers in Immunology*, 10.

Hanahan, D., & Weinberg, R. A. (2000). The Hallmarks of Cancer. *Cell*, 100(1), 57–70.

Hanahan, D., & Weinberg, R. A. (2011). Hallmarks of Cancer: The Next Generation. *Cell,* 144(5), 646-674.

Hassanpour, S. H., & Dehghani, M. (2017). Review of Cancer from Perspective of Molecular. *Journal of Cancer Research and Practice*, 4(4), 127-129.

Hewitt E. W. (2003). The MHC class I antigen presentation pathway: strategies for viral immune evasion. *Immunology*, 110(2), 163–169.

Ilyas, M., & Tomlinson, I. P. M. (1996). Genetic pathways in Colorectal Cancer. *Histopathology*, 28(5), 389-399.

Inagaki-Ohara, K., Kondo, T., Ito, M., & Yoshimura, A. (2013). SOCS, inflammation, and cancer. *JAK-STAT*, 2(3).

Ito, D., Imai, Y., Ohsawa, K., Nakajima, K., Fukuuchi, Y., & Kohsaka, S. (1998). Microglia-specific localisation of a novel calcium binding protein, Iba1. *Brain research. Molecular Brain Research*, 57(1), 1–9.

Jayasingam, S. D., Citartan, M., Thang, T. H., Mat Zin, A. A., & Ang, K. C. (2019). Evaluating the Polarization of Tumour-Associated Macrophages into M1 and M2 Phenotypes in Human Cancer Tissue: Technicalities and Challenges in Routine Clinical Practice. *Frontiers in Oncology*, 9.

Jiang, M., Liu, P., Yu, W., Liu, T., & Yu, J. (2017). Dysregulation of SOCS-Mediated Negative Feedback of Cytokine Signalling in Carcinogenesis and Its Significance in Cancer Treatment. *Frontiers in Immunology*, 8.

Jiang, N., Zhang, L., Zhao, G., Lin, J., Wang, Q., Xu, Q., Li, C., Hu, L., Peng, X., Yu, F., & Xu, M. (2020). Indoleamine 2,3-Dioxygenase Regulates Macrophage Recruitment, Polarization and Phagocytosis in *Aspergillus Fumigatus* Keratitis. *Investigative Ophthalmology & Visual Science*, 61(8).

Jochems, C., Fantini, M., Fernando, R. I., Kwilas, A. R., Donahue, R. N., Lepone, L. M., Grenga, I., Kim, Y. S., Brechbiel, M. W., Gulley, J. L., Madan, R. A., Heery, C. R., Hodge, J. W., Newton, R., Schlom, J., & Tsang, K. Y. (2016). The IDO1 selective inhibitor Epacadostat enhances dendritic cell immunogenicity and lytic ability of tumour antigen-specific T cells. *Oncotarget*, *7*(25), 37762–37772.

Kang, S., Tanaka, T., Narazaki, M., & Kishimoto, T. (2019). Targeting Interleukin-6 signalling in clinic. *Immunity*, 50(4), 1007-1023.

Kazemi, M. H., Sadri, M., Najafi, A., Rahimi, A., Baghernejadan, Z., Khorramdelazad, H., & Falak, R. (2022). Tumour-infiltrating lymphocytes for treatment of solid tumours:

It takes two to tango. *Frontiers in Immunology*, 13, 1-23.

Kershaw, N. J., Laktyushin, A., Nicola, N. A., & Babon, J. J. (2014). Reconstruction of an active SOCS3-based E3 ubiquitin ligase complex in vitro: identification of the active components and JAK2 and gp130 as substrates. *Growth Factors (Chur, Switzerland)*, 32(1), 1–10.

Kuipers, E. J., Grady, W. M., Lieberman, D., Seufferlein, T., Sung, J. J., Boelens, P. G., van de Velde, C. J., & Watanabe, T. (2015). Colorectal Cancer. *Nature Reviews. Disease Primers*, 1, 15065.

Kumar, A., Gautam, V., Sandhu, A., Rawat, K., Sharma, A., & Saha, L. (2023). Current and emerging therapeutic approaches for colorectal cancer: A comprehensive review. *World Journal of Gastrointestinal Surgery*, 15(4), 495–519.

Kumari, N., Dwarakanath, B.S., Das, A & Bhatt A. N. (2016). Role of interleukin-6 in cancer progression and therapeutic resistance. *Tumour Biology,* 37, 11553–11572.

Lánczky, A., & Győrffy, B. (2021). Web-based survival analysis tool tailored for medical research (KMplot): Development and Implementation. *Journal of Medical Internet Research*, 23(7).

Lee, G. K., Park, H. J., Macleod, M., Chandler, P., Munn, D. H., & Mellor, A. L. (2002). Tryptophan deprivation sensitizes activated T cells to apoptosis prior to cell division. *Immunology*, 107(4), 452–460.

Lesniak, W. G., Jyoti, A., Mishra, M. K., Louissaint, N., Romero, R., Chugani, D. C., Kannan, S., & Kannan, R. M. (2013). Concurrent quantification of tryptophan and its major metabolites. *Analytical Biochemistry*, 443(2), 222.

Lin, J. S., Piper, M. A., Perdue, L. A., Rutter, C., Webber, E. M., O'Connor, E., Smith, N., & Whitlock, E. P. (2016). Screening for colorectal cancer: A systematic review for the U.S. preventive services task force. Agency for Healthcare Research and Quality (US).

Liu, M., Wang, X., Wang, L., Ma, X., Gong, Z., Zhang, S & Li, Y. (2018). Targeting the IDO1 pathway in cancer: from bench to bedside. *Journal of Hematology & Oncology,* 11.

Martinez, J., & Parker, M., Fultz, K., Ignatenko, N., & Gerner, E. (2003). Molecular Biology of Cancer. Burger's Medicinal Chemistry and Drug Discovery Sixth Edition, Volume 5: Chemotherapeutic Agents. 50.

Mbongue, J. C., Nicholas, D. A., Torrez, T. W., Kim, N. S., Firek, A. F., & Langridge, W. H. (2015). The role of Indoleamine 2, 3-Dioxygenase in immune suppression and autoimmunity. *Vaccines*, 3(3), 703–729.

Mellor, A. L. & Munn, D. H. (1999). Tryptophan catabolism and T-cell tolerance: immunosuppression by starvation? *Immunology Today*, 20(10), 469-473.

Menon, A. G., Morreau, H., Tollenaar, R. A., Alphenaar, E., Van Puijenbroek, M., Putter, H., Janssen-Van Rhijn, C. M., Van De Velde, C. J., Fleuren, G. J., & Kuppen, P. J. (2002). Down-regulation of HLA-A expression correlates with a better prognosis in colorectal cancer patients. *Laboratory Investigation; a Journal of Technical Methods and Pathology*, 82(12), 1725–1733.

Mikkelsen, H. B., Huizinga, J. D., Larsen, J. O., & Kirkeby, S. (2017). Ionized calcium binding adaptor molecule 1 positive macrophages and HO-1 up-regulation in intestinal muscularis resident macrophages. *Anatomical Record (Hoboken, N.j. :2007)*, 300(6), 1114-1122.

Mills, C. D., Kincaid, K., Alt, J. M., Heilman, M. J., & Hill, A. M. (2000). M-1/M-2 macrophages and the Th1/Th2 paradigm. *Journal of Immunology (Baltimore, Md. :1950)*, 164(12), 6166–6173.

Mitchell, T. C., Hamid, O., Smith, D. C., Bauer, T. M., Wasser, J. S., Olszanski, A. J., Luke, J. J., Balmanoukian, A. S., Schmidt, E. V., Zhao, Y., Gong, X., Maleski, J., Leopold, L., & Gajewski, T. F. (2018). Epacadostat Plus Pembrolizumab in Patients With Advanced Solid Tumours: Phase I Results from a Multicentre, Open-Label Phase I/II Trial (ECHO-202/KEYNOTE-037). *Journal of Clinical Oncology: Official Journal of the*

American Society of Clinical Oncology, 36(32), 3223–3230.

Moffett, J. R., & Namboodiri, M. A. (2003). Tryptophan and the immune response. *Immunology and Cell Biology*, *81*(4), 247–265.

Munn, D. H., Sharma, M. D., Hou, D., Baban, B., Lee, J. R., Antonia, S. J., Messina, J. L., Chandler, P., Koni, P. A., & Mellor, A. L. (2004). Expression of indoleamine 2,3 dioxygenase by plasmacytoid dendritic cells in tumour-draining lymph nodes. *The Journal of Clinical Investigation*, 114(2), 280–290.

Murakami, M., Ohtani, T., & Hirano, T. (2014). Interleukin-6. *Reference Module in Biomedical Sciences*.

National Cancer Institute. (2022). Immune Checkpoint Inhibitors. [Online]. National Cancer Institute. Last Updated: 2022. Available at: https://www.cancer.gov/about cancer/treatment/types/immunotherapy/checkpoint-inhibitors [Accessed 31 December 2023].

National Cancer Institute. (2022). The Genetics of Cancer. [Online]. National Cancer Institute. Last Updated: 17 August 2022. Available at: https://www.cancer.gov/about-cancer/causes-prevention/genetics [Accessed 4 January 2023].

National Cancer Institute. (2023). Colon. [Online]. National Cancer Institute. Available at: https://www.cancer.gov/publications/dictionaries/cancer-terms/def/colon [Accessed 9 May 2023].

National Cancer Institute. (2023). IDO1. [Online]. National Cancer Institute. Available at: https://portal.gdc.cancer.gov/genes/ENSG00000131203 [Accessed 3 December 2023].

Neuwirt, H., Puhr, M., Cavarretta, I. T., Mitterberger, M., Hobisch, A., & Culig, Z. (2007). Suppressor of cytokine signalling-3 is up-regulated by androgen in prostate cancer cell lines and inhibits androgen-mediated proliferation and secretion. *Endocrine-related cancer*, *14*(4), 1007–1019.

Orabona, C., Pallotta, M. T., Volpi, C., Fallarino, F., Vacca, C., Bianchi, R., Belladonna, M. L., Fioretti, M. C., Grohmann, U., & Puccetti, P. (2008). SOCS3 drives proteasomal degradation of indoleamine 2,3-dioxygenase (IDO) and antagonizes IDO-dependent tolerogenesis. *Proceedings of the National Academy of Sciences*, 105(52), 20828-20833.

Parang, B., Barret, C. W., & Williams, C. S. (2016). AOM/DSS Model of Colitis Associated Cancer. *Methods in Molecular Biology (Clifton, N.J.)*, 1422, 297.

Pernot, S., Terme, M., Voron, T., Colussi, O., Marcheteau, E., Tartour, E., & Taieb, J. (2014). Colorectal cancer and immunity: what we know and perspectives. *World Journal of Gastroenterology*, 20(14), 3738–3750.

Qin, H., Holdbrooks, A. T., Liu, Y., Reynolds, S. L., Yanagisawa, L. L., & Benveniste, E. N. (2012). SOCS3 deficiency promotes M1 macrophage polarization and inflammation. *Journal of Immunology (Baltimore, Md. : 1950),* 189(7), 3439–3448.

Richard, D. M., Dawes, M. A., Mathias, C. W., Acheson, A., Hill-Kapturczak, N., & Dougherty, D. M. (2009). L-Tryptophan: Basic Metabolic Functions, Behavioral Research and Therapeutic Indications. *International Journal of Tryptophan Research : IJTR*, *2*, 45-60.

Rico-Bautista, E., Flores-Morales, A., & Fernández-Pérez, L. (2006). Suppressor of cytokine signalling (SOCS) 2, a protein with multiple functions. *Cytokine & Growth Factor Reviews*, 17(6), 431–439.

Rigby, R. J., Simmons, J. G., Greenhalgh, C. J., Alexander, W. S., & Lund, P. K. (2007). Suppressor of cytokine signalling 3 (SOCS3) limits damage-induced crypt hyper proliferation and inflammation-associated tumorigenesis in the colon. *Oncogene,* 26(33), 4833-41.

Rosenberg, S. A., & Restifo, N. P. (2015). Adoptive cell transfer as personalized immunotherapy for human cancer. *Science (New York, N.Y.)*, 348(6230), 62–68.

Rose-John, S. (2018). Interleukin-6 family cytokines. *Cold Spring Harbor Perspectives in Biology*, 10(2).

Routy, J. P., Routy, B., Graziani, G. M., & Mehraj, V. (2016). The Kynurenine Pathway Is a Double-Edged Sword in Immune-Privileged Sites and in Cancer: Implications for Immunotherapy. *International Journal of Tryptophan Research: IJTR*, 9, 67–77.

Schmidt-Arras, D., Müller, M., Stevanovic, M., Horn, S., Schütt, A., Bergmann, J., Wilkens, R., Lickert, A., & Rose-John, S. (2014). Oncogenic deletion mutants of gp130 signal from intracellular compartments. *Journal of Cell Science*, 127(Pt 2), 341–353.

Schneider, M. R., Hoeflich, A., Fischer, J. R., Wolf, E., Sordat, B., & Lahm, H. (2000). Interleukin-6 stimulates clonogenic growth of primary and metastatic human colon carcinoma cells. *Cancer Letters*, 151(1), 31–38.

Seif, F., Khoshmirsafa, M., Aazami, H., Mohsenzadegan, M., Sedighi, G., & Bahar, M. (2017). The role of JAK-STAT signalling pathway and its regulators in the fate of T-helper cells. *Cell Communication & Signalling*, 15(1), 23.

Sellitto, A., Galizia, G., De Fanis, U., Lieto, E., Zamboli, A., Orditura, M., De Vita, F., Giunta, R., Lucivero, G., & Romano, C. (2011). Behaviour of circulating CD4+CD25+Foxp3+ regulatory T cells in colon cancer patients undergoing surgery. *Journal of Clinical Immunology*, 31(6), 1095–1104.

Shaw, E. J., Smith, E. E., Whittingham-Dowd, J., Hodges, M. D., Else, K. J., & Rigby, R. J. (2017). Intestinal epithelial suppressor of cytokine signalling 3 (SOCS3) impacts on mucosal homeostasis in a model of chronic inflammation. *Immunity, inflammation and disease*, 5(3), 336–345.

Sourav, P & Girdhari, L. (2017). The Molecular Mechanism of Natural Killer Cells Function and Its Importance in Cancer Immunotherapy. *Frontiers in Immunology*, 8(1124), 1-15.

Struckmeier, A. K., Radermacher, A., Fehrenz, M., Bellin, T., Alansary, D., Wartenberg, P., Boehm, U., Wagner, M., Scheller, A., Hess, J., Moratin, J., Freudlsperger, C., Hoffmann, J., Thurner, L., Roemer, K., Freier, K., & Horn, D. (2023). IDO1 is highly expressed in macrophages of patients in advanced tumour stages of oral squamous cell carcinoma. *Journal of Cancer Research and Clinical Oncology,* 149, 3623–3635.

Sucher, R., Kurz, K., Weiss, G., Margreiter, R., Fuchs, D., & Brandacher, G. (2010). IDO-Mediated Tryptophan Degradation in the Pathogenesis of Malignant Tumour Disease. *International Journal of Tryptophan Research: IJTR*, *3*, 113-120.

Suwannasom, N., Smuda, K., Kloypan, C., Kaewprayoon, W., Baisaeng, N., Boonla, C., Georgieva, R., & Bäumler, H. (2019). Detection of CD33 expression on monocyte surface is influenced by phagocytosis and temperature. *General Physiology and Biophysics*, 38(5), 369–378.

Tanaka, T., Narazaki, M., & Kishimoto, T. (2014). IL-6 in inflammation, immunity, and disease. *Cold Spring Harbor Perspectives in Biology*, 6(10).

Tanchot, C., Terme, M., Pere, H., Tran, T., Benhamouda, N., Strioga, M., Banissi, C., Galluzzi, L., Kroemer, G., & Tartour, E. (2013). Tumour-infiltrating regulatory T cells: phenotype, role, mechanism of expansion in situ and clinical significance. *Cancer*

Microenvironment: Official Journal of the International Cancer Microenvironment Society, 6(2), 147–157.

Tang, K., Wu, YH., Song, Y., & Yu, B. (2021). Indoleamine 2,3-dioxygenase 1 (IDO1) inhibitors in clinical trials for cancer immunotherapy. *Journal of Hematology & Oncology,* 14, 68.

Terme, M., Fridman, W. H., & Tartour, E. (2013). NK cells from pleural effusions are potent antitumor effector cells. *European Journal of Immunology*, 43(2), 331–334.

Tirosh, I., Izar, B., Prakadan, S. M., Treacy, D., Trombetta, J. J., Rotem, A., Rodman, C., Lian, C., Murphy, G., Fallahi-Sichani, M., Dutton-Regester, K., Lin, R., Cohen, O., Shah, P., Lu, D., Genshaft, A. S., Hughes, T. K., K. Ziegler, C. G., Kazer, S. W., Garraway, L. A. (2016). Dissecting the multicellular ecosystem of metastatic melanoma by single cell RNA-seq. *Science (New York, N.Y.)*, 352(6282), 189.

Vacchelli, E., Aranda, F., Eggermont, A., Sautès-Fridman, C., Tartour, E., Kennedy, E. P., Platten, M., Zitvogel, L., Kroemer, G., & Galluzzi, L. (2014). Trial watch: IDO inhibitors in cancer therapy. *Oncoimmunology*, 3(10), 957994.

Wang, N., Liang, H., & Zen, K. (2014). Molecular mechanisms that influence the macrophage M1-M2 polarization balance. *Frontiers in Immunology*, 5, 1664-3224.

Wang, S., Wu, J., Shen, H., & Wang, J. (2020). The prognostic value of IDO expression in solid tumours: a systematic review and meta-analysis. *BMC Cancer,* 20, 471.

Wang, X., Wang, H., Wang, H., Zhang, F., Wang, K., Guo, Q., Zhang, G., Cai, S., & Du, J. (2014). The role of indoleamine 2,3-dioxygenase (IDO) in immune tolerance: Focus on macrophage polarization of THP-1 cells. *Cellular Immunology*, 289(1-2), 42-48.

Wei, W., Ning, C., Huang, J., Wang, G., Lai, J., Han, J., He, J., Zhang, H., Liang, B., Liao, Y., Le, T., Luo, Q., Li, Z., Jiang, J., Ye, L., & Liang, H. (2021). *Talaromyces marneffei* promotes M2-like polarization of human macrophages by downregulating SOCS3 expression and activating the TLR9 pathway. *Virulence*, 12(1), 1997–2012.

White, M. C., Holman, D. M., Boehm, J. E., Peipins, L. A., Grossman, M., & Henley, S. J. (2014). Age and cancer risk: a potentially modifiable relationship. *American Journal of Preventive Medicine*, 46(3), 7–15.

Whittingham-Dowd, J., Jewers, C., Eastoe, L., Bultler-Craft, A., Worthington, J., Rigby, R. (In Preparation, 2024). Role of Suppressor of Cytokine Signalling 3 (SOCS3) in the tumour microenvironment and resistance to IDO inhibitor therapy.

Wilson, H. M. (2014). SOCS Proteins in Macrophage Polarization and Function. *Frontiers in Immunology*, *5*.

World Health Organization. (2022). Cancer. [Online]. World Health Organization. Last Updated: 3 February 2022. Available at: https://www.who.int/news-room/fact sheets/detail/cancer [Accessed 4 January 2023].

Xu, J., Gu, Y., Wang, Z., Jin, Y., Wen, M., Ma, C., Tang, J., Mao, W., Qian, J., & Lin, J. (2020). The M2 macrophage marker CD206: A novel prognostic indicator for acute myeloid leukaemia. *Oncoimmunology*, 9(1).

Xu, M., Wang, Y., Xia, R., Wei, Y., & Wei, X. (2021). Role of the CCL2-CCR2 signalling axis in cancer: Mechanisms and therapeutic targeting. *Cell Proliferation*, 54(10), 13115.

Yan, C., Ward, P. A., Wang, X., & Gao, H. (2013). Myeloid depletion of SOCS3 enhances LPS-induced acute lung injury through CCAAT/enhancer binding protein δ pathway. *FASEB Journal : Official Publication of the Federation of American Societies for Experimental Biology*, 27(8), 2967–2976.

Yao, Y., Xu, X., & Jin, L. (2019). Macrophage polarisation in physiological and pathological pregnancy. *Frontiers in Immunology*, 10, 1664-3224.

Yoshimura, A., Naka, T., & Kubo, M. (2007). SOCS proteins, cytokine signalling and immune regulation. *Nature Reviews Immunology,* 7(6), 454–465.

Yoshida, K., Taga, T., Saito, M., Suematsu, S., Kumanogoh, A., Tanaka, T., Fujiwara, H., Hirata, M., Yamagami, T., Nakahata, T., Hirabayashi, T., Yoneda, Y., Tanaka, K., Wang, W. Z., Mori, C., Shiota, K., Yoshida, N., & Kishimoto, T. (1996). Targeted disruption of gp130, a common signal transducer for the interleukin 6 family of cytokines, leads to myocardial and hematological disorders. *Proceedings of the National Academy of Sciences of the United States of America*, 93(1), 407–411.

Yu, F., Jiang, W., Zhang, L., & Jiang, N. (2023). IDO Regulates Macrophage Functions by Inhibiting the CCL2/CCR2 Signalling Pathway in Fungal Keratitis. *Cornea*, 42(8), 1005–1015.

Zhai, L., Bell, A., Ladomersky, E., Lauing, K. L., Bollu, L., Sosman, J. A., Zhang, B., Wu, J. D., Miller, S. D., Meeks, J. J., Lukas, R. V., Wyatt, E., Doglio, L., Schiltz, G. E., McCusker, R. H., & Wainwright, D. A. (2020). Immunosuppressive IDO in cancer: mechanisms of action, animal models, and targeting strategies. *Frontiers in*

Immunology, 11, 1185.